Developmental Biology 450 (2019) 141–154

Contents lists available at ScienceDirect

Developmental Biology

journal homepage: www.elsevier.com/locate/developmentalbiology

GLI3 repressor but not GLI3 activator is essential for mouse eye patterning and morphogenesis

Antonia Wiegering [a], Patrick Petzsch [b], Karl Köhrer [b], Ulrich Rüther [a], Christoph Gerhardt [a,*]

[a] Institute for Animal Developmental and Molecular Biology, Heinrich Heine University, 40225 Düsseldorf, Germany
[b] Biological and Medical Research Center (BMFZ), Genomics and Transcriptomics Laboratory (GTL), Heinrich Heine University, 40225 Düsseldorf, Germany

ARTICLE INFO

Keywords:
Eye development
Lens
Retina
Hedgehog
WNT
DKK
β-CATENIN

ABSTRACT

Since 1967, it is known that the loss of GLI3 causes very severe defects in murine eye development. GLI3 is able to act as a transcriptional activator (GLI3-A) or as a transcriptional repressor (GLI3-R). Soon after the discovery of these GLI3 isoforms, the question arose which of the different isoforms is involved in eye formation – GLI3-A, GLI3-R or even both. For several years, this question remained elusive. By analysing the eye morphogenesis of *Gli3*$^{XtJ/XtJ}$ mouse embryos that lack GLI3-A and GLI3-R and of *Gli3*$^{\Delta 699/\Delta 699}$ mouse embryos in which only GLI3-A is missing, we revealed that GLI3-A is dispensable in vertebrate eye formation. Remarkably, our study shows that GLI3-R is sufficient for the creation of morphologically normal eyes although the molecular setup deviates substantially from normality. In depth-investigations elucidated that GLI3-R controls numerous key players in eye development and governs lens and retina development at least partially via regulating WNT/β-CATENIN signalling.

1. Introduction

Vision is the dominant sense of most vertebrates. To study vertebrate eye development, the mouse is one of the most used organisms. Eye development in mice begins with the formation of the eye field at embryonic day (E)8.0 and of the optic pit at E8.5 (Fuhrmann, 2010). Afterwards, the optic pit evaginates to give rise to the optic vesicle. In midgestation, the formation of the lens placode is initiated by the optic vesicle. Concomitantly, the optic vesicle invaginates to form the bilayered optic cup. The inner layer becomes the neural retina, while the outer layer turns to retinal pigment epithelium. The optic cups are linked to the diencephalon by the optic stalks. A proximal extension of the optic vesicle invagination which includes the ventral portion of the optic stalk causes a transient groove (optic fissure). Through this opening, mesenchymal cells migrate into the eye chamber to give rise to hyaloid vessels which represent the main blood supply for the eye (Barishak, 1992). After this migration event, the optic fissure closes. The so called optic disc (blind spot of the retina) is defined as the region of the retina where the ganglion cell axons exit the eye. Thus, these axons run together at the optic disc being a part of the optic nerve. Any deviations from these development processes result in the appearance of congenital eye defects.

Human congenital eye defects appear at a frequency of about 0.05% of live births (Ludwig and Czyz, 2017). Several of these defects like anophthalmia (loss of one or both eyes), microphthalmia (one or both eyes are reduced in size), coloboma (a portion of a structure of the eye e.g. iris, retina, lens or lid is missing and leads to a gap in the eye structure) or aphakia (absence of the lens in one or both eyes) are associated with blindness (de Verdier et al., 2017; Gogate et al., 2011; Sano et al., 2018; Verma and Fitzpatrick, 2007). In view of the large number of blind children (an estimated 1.4 million of the children worldwide) and based on that congenital eye defects are the leading cause of blindness, great effort has been made to identify factors that play a prominent role in the development of congenital eye defects (Graw, 2003; Li and Lin, 2013; Solebo et al., 2017). In search of the molecular reasons underlying congenital eye defects, genetic screens revealed that patients suffering from these defects often bear mutations in *ALDH1A3*, *CRYAB*, *FOXE3*, *GJA8*, *ODZ3*, *OTX2*, *PAX2, PAX6*, *SIX3*, *SMOC1*, *SOX1* or *SOX2* (Aldahmesh et al., 2012; Berry et al., 2001; Ceroni et al., 2018; Graw, 2009a,b; Hever et al., 2006; Jiao et al., 2015; Khan et al., 2010; Khan et al., 2015; Kumar et al., 2011; Medina-Martinez and Jamrich, 2007; Pineda-Alvarez et al., 2011; Reis and Semina, 2015; Traboulsi, 1998; Williamson and FitzPatrick, 2014). Moreover, it was shown that vertebrate eye development requires a complex interplay of various signalling transduction cascades (Cvekl and Zhang, 2017; Fuhrmann, 2010; Gregory-Evans et al.,

* Corresponding author.
E-mail addresses: Antonia.Wiegering@hhu.de (A. Wiegering), Patrick.Petzsch@hhu.de (P. Petzsch), Koehrer@hhu.de (K. Köhrer), ruether@hhu.de (U. Rüther), Christoph.Gerhardt@hhu.de (C. Gerhardt).

https://doi.org/10.1016/j.ydbio.2019.02.018
Received 9 November 2018; Received in revised form 12 February 2019; Accepted 15 February 2019
Available online 3 April 2019

2013; Kumar, 2001; Lee et al., 2018; Russell, 2003). Examples of these signalling cascades are the WNT/β-CATENIN and the Hedgehog (HH) signalling pathway.

Canonical WNT/β-CATENIN signalling is initiated by the binding of the WNT ligand to a receptor complex consisting of Frizzled (FZD) and the Low-density lipoprotein receptor-related proteins 5 and 6 (LRP5 and LRP6) (Bhanot et al., 1996; Pinson et al., 2000; Tamai et al., 2000; Wehrli et al., 2000). Subsequently, β-CATENIN translocates from the cytoplasm into the nucleus where it interacts with the TCF/LEF family of transcription factors and thereby induces the expression of WNT/β-CATENIN target genes (Willert and Nusse, 1998). Upon binding of DKK1 to LRP5/6, the formation of the WNT/FZD/LRP5/6 complex and hence the activation of WNT signalling is inhibited (Bafico et al., 2001; Mao et al., 2001; Semënov et al., 2001). In this case, cytoplasmic β-CATENIN becomes phosphorylated, ubiquitinated and finally degraded. In the context of eye development, WNT/β-CATENIN signalling plays an important role in for example regulating the formation of the optic cup, ocular tissue patterning and supporting the differentiation of the retinal pigment epithelium (Fuhrmann, 2008, 2010; Fujimura, 2016). At the molecular level, WNT/β-CATENIN signalling regulates the expression of e.g. *Otx2*, *Six3*, *Sox2* and *Vax2* in eye organogenesis (Hägglund et al., 2013).

HH signalling plays an important role in the patterning of the optic cup and in the closure of the optic fissure (Amato et al., 2004; Take-uchi et al., 2003). The HH signalling cascade starts with the binding of the HH ligand to its receptor Patched (PTCH). Due to this binding, SMO is able to activate members of the Glioblastoma (GLI) family of zinc finger transcription factors named GLI2 and GLI3. Both proteins mediate HH signalling and can function as activators or repressors of HH target gene expression (Ruiz i Altaba, 1999b; Sasaki et al., 1999). By doing so, GLI2 and GLI3 play crucial roles ensuring the proper formation of numerous structures and organs (Ingham and McMahon, 2001; Ruiz i Altaba, 1999a; Ruiz i Altaba et al., 2003; Ruiz i Altaba et al., 2002). To take up their work as transcriptional repressors, GLI2 and GLI3 are proteolytically processed by the proteasome (Li et al., 2011; Pan et al., 2006; Wang et al., 2000). Although both repressors play important roles in vertebrate development (Gerhardt et al., 2016b), the repressor form of GLI3 was described to be predominant (Bai et al., 2004; Bangs and Anderson, 2017; Jacob and Briscoe, 2003; Rallu et al., 2002). $Gli3^{XtJ/XtJ}$ homozygous mutant mice lack GLI3 (Schimmang et al., 1992) and display a plethora of developmental defects from which they die during embryogenesis (Franz and Besecke, 1991; Furimsky and Wallace, 2006; Johnson, 1967). These defects include, inter alia, eye malformations which have been described extensively and vary widely in their severity (Franz and Besecke, 1991; Johnson, 1967). It is a long-lasting and still open question how GLI3 regulates eye formation. In this context, it would be a big step forward to reveal which isoform of the GLI3 protein is pivotal for eye formation - the GLI3 activator (GLI3-A), the GLI3 repressor (GLI3-R) or both. Since the general view is that GLI3 functions mainly as a transcriptional repressor, it was previously proposed that the repressor form of GLI3 is essential for eye development (Zaki et al., 2006). However, it is known that GLI3-A is involved in some aspects of vertebrate development, e.g. in limb digit and neural tube patterning as well as in genital development (Bai et al., 2004; He et al., 2016; Lei et al., 2004; Wang et al., 2007). The eye phenotypes described in mouse mutants of the positive HH signalling regulators SHH and SMO suggest that GLI2-A and GLI3-A play important roles in vertebrate eye development. *Shh*-negative mouse embryos are cyclopic and their eyes exhibit a disrupted formation of the optic stalk and an impaired development of the neural retina (Chiang et al., 1996; Kim and Lemke, 2006). Conditional deletion of SMO in the eye results in lens defects, corneal defects and loss of the complete eye structure (Choi et al., 2014; Zhao et al., 2010). With regard to GLI3, the *Shh* and *Smo* mutants are supposed to have less GLI3-A but an unaltered or even higher amount of GLI3-R. Based on this, one can hypothesise that GLI3-A is needed for proper eye development in vertebrates. In addition of the decreased GLI3-A amount, it is also expected that the amount of GLI2-A is reduced in $Shh^{-/-}$ and $Smo^{-/-}$ murine eyes. Since GLI2 functions as a stronger activator in the HH signalling cascade than GLI3 (Sasaki et al., 1999), it is also conceivable that these defects develop due to the loss of GLI2-A rather than to the loss of GLI3-A. However, $Gli2^{-/-}$ mouse eyes show no eye defects except of a slightly shortened optic stalk (Furimsky and Wallace, 2006) suggesting that not GLI2-A but GLI3-A might be decisive for vertebrate eye development.

All previous studies that investigated the relationship between GLI3 and eye development used $Gli3^{XtJ}$ mutant mouse embryos and hence worked under conditions in which GLI3 was completely missing (Aoto et al., 2002; Burnett et al., 2017; Franz and Besecke, 1991; Furimsky and Wallace, 2006; Johnson, 1967; Lieven and Rüther, 2011; Lupu et al., 2018; Zaki et al., 2006). Thus, these former investigations did not allow to discriminate between the effects of GLI3-A and the effects of GLI3-R on eye development. In our study, we used $Gli3^{\Delta 699}$ mutant mice, which express a constitutively active GLI3-R protein (Böse et al., 2002), to distinguish between the function of GLI3-A and GLI3-R in vertebrate eye development. We compared the eye phenotypes of $Gli3^{XtJ/XtJ}$ and $Gli3^{\Delta 699/\Delta 699}$ mouse embryos at E14.5 and E18.5. While $Gli3^{XtJ/XtJ}$ embryos exhibit eye defects varying from microphthalmia to anophthalmia, $Gli3^{\Delta 699/\Delta 699}$ embryos did not display any morphological eye defects demonstrating that GLI3-R but not GLI3-A is critical for eye development. To investigate the consequences of the different mutations molecularly, we performed a microarray analysis that revealed a higher number of expressionally altered genes in $Gli3^{\Delta 699/\Delta 699}$ than in $Gli3^{XtJ/XtJ}$ embryonic eyes. However, this analysis points out that a large number of factors which represent main protagonists in eye development showed a changed expression in $Gli3^{XtJ/XtJ}$ but not in $Gli3^{\Delta 699/\Delta 699}$embryonic eyes. To unveil how GLI3-R controls eye morphogenesis, we carried out in situ hybridisation and immunofluorescence studies at E12.5. These examinations showed that the loss of GLI3-R affects several key players of eye development. Most of these factors are associated with WNT/β-CATENIN signalling. In summary, our data reveal that the activator form of GLI3 is dispensable for proper eye morphogenesis, while the repressor form of GLI3 governs vertebrate eye development at least partially via controlling WNT/β-CATENIN signalling.

2. Results

Previously, it was shown that GLI3 is present in embryonic mouse eyes and plays a role in their development (Aoto et al., 2002; Choi et al., 2014; Franz and Besecke, 1991; Furimsky and Wallace, 2006; Johnson, 1967; Zaki et al., 2006). The GLI3 full-length protein can be modified either into a transcriptional activator or a transcriptional repressor (Sasaki et al., 1999). Until now, it is unknown if both forms of the GLI3 protein are involved in eye development or whether only one of these forms is sufficient for proper eye formation. To discriminate between the functions of GLI3-A and GLI3-R, we generated $Gli3^{\Delta 699}$-mutant mice which produce a constitutive active GLI3-R protein (Böse et al., 2002). We assessed the roles of GLI3-A and GLI3-R in eye morphogenesis by comparing the eye phenotypes of $Gli3^{\Delta 699/\Delta 699}$ and $Gli3^{XtJ/XtJ}$ mouse embryos at E14.5 and E18.5.

2.1. GLI3-A is dispensable for proper eye morphogenesis

In line with previous reports about the mutant eye phenotype of $Gli3^{XtJ/XtJ}$ mouse embryos (Franz and Besecke, 1991; Johnson, 1967), we observed microphthalmia, anophthalmia, coloboma, lens stalk persistence, hyaloid hypercellularity or aphakia in the absence of GLI3 (Fig. 1A–D). As described before (Franz and Besecke, 1991), we also found phenotypically normal $Gli3^{XtJ/XtJ}$ eyes (Fig. 1A and B). We detected eye defects in 71% (27 out of 38) of all analysed $Gli3^{XtJ/XtJ}$ mouse embryos at E14.5 and E18.5. Remarkably, 50% (11 out of 22) of all analysed $Gli3^{XtJ/XtJ}$ eyes at E14.5 showed phenotypical defects, while 100% (16 out of 16) of all analysed $Gli3^{XtJ/XtJ}$ eyes at E18.5 exhibited morphological abnormalities (Table 1) indicating that GLI3 deficiency might affect processes in eye development even after E14.5 and lead to malformations

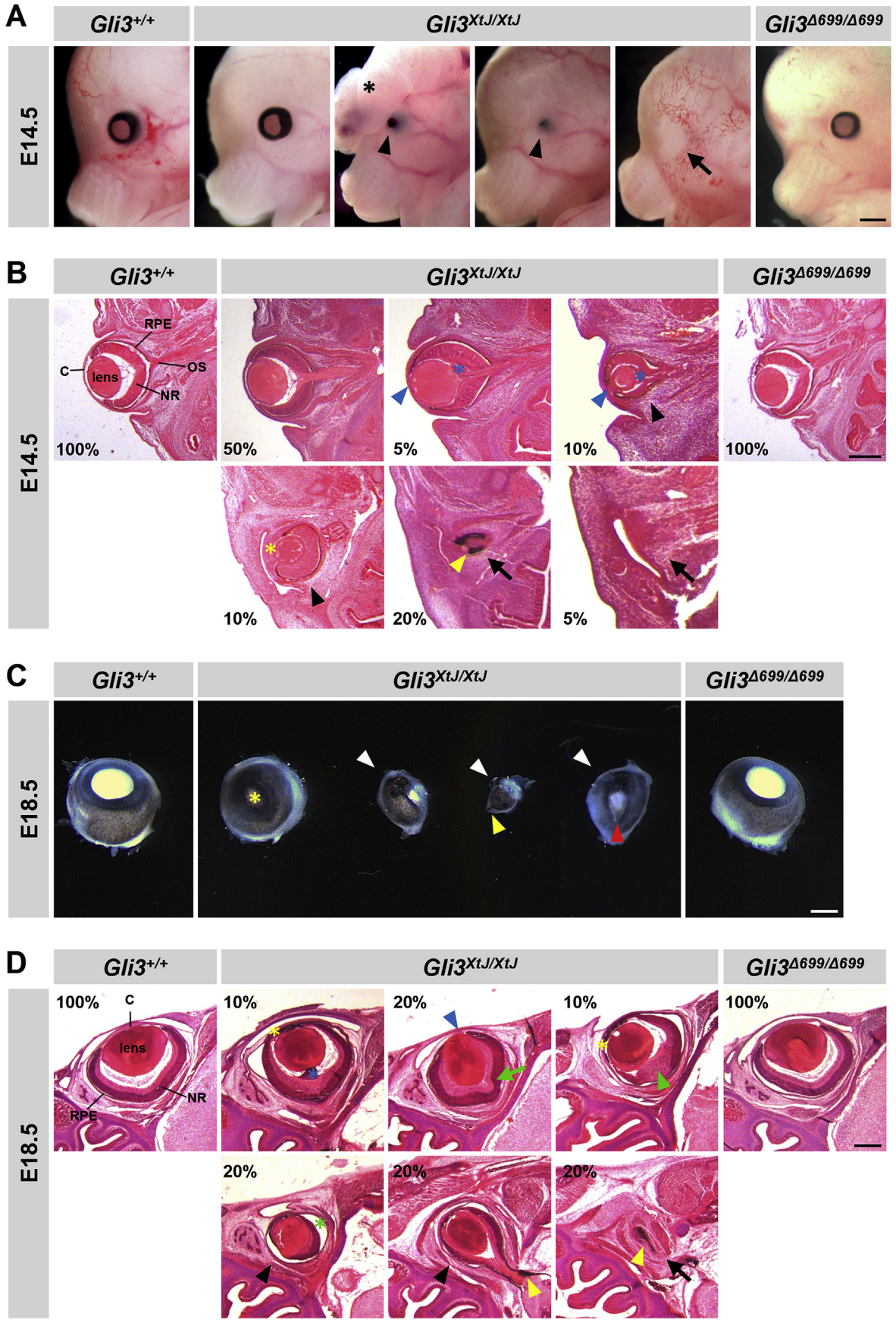

(caption on next page)

Fig. 1. *Gli3*$^{XtJ/XtJ}$ mutant mouse embryos display a variety of eye defects while *Gli3*$^{\Delta699/\Delta699}$ mutant eyes are phenotypically normal. (A) Morphology of heads from embryos at embryonic stage E14.5. WT and *Gli3*$^{\Delta699/\Delta699}$ embryos show no eye defects. *Gli3*$^{XtJ/XtJ}$ mutant embryos display normal shaped eyes or several defects like microphthalmia (indicated by black arrowheads) or anophthalmia (indicated by black arrow). The asterisk indicates the presence of exencephaly. The scale bar represents a length of 500 µm. (B) HE staining of embryonic eyes at embryonic stage E14.5. WT (n = 21) and *Gli3*$^{\Delta699/\Delta699}$ (n = 14) embryos show no eye defects. *Gli3*$^{XtJ/XtJ}$ embryos (n = 22) exhibit normally shaped eyes (50%) or show different defects (50%). In most of the cases *Gli3*$^{XtJ/XtJ}$ embryos display a microphthalmia (indicated by black arrowheads), which can be combined with other abnormalities like a lens stalk persistence (indicated by blue arrowheads) or a hyaloid hyper cellularity (indicated by blue asterisks). Additional defects in the formation of the anterior and posterior eye chamber (indicated by yellow asterisk) as well as the loss of several eye structures like the lens (aphakia) can be observed. Moreover, a total absence of the eye (anophthalmia; indicated by black arrow) or just remnants of eye structures like pigmented cells (indicated by yellow arrowhead) and extraocular muscles can be monitored in *Gli3*$^{XtJ/XtJ}$ embryos. Percentages indicate the defect frequencies. The scale bar represents a length of 250 µm. C, cornea; NR, neural retina; ON, optic nerve; RPE, retinal pigmented epithelium. (C) Morphology of eyes from embryos at embryonic stage E18.5. WT and *Gli3*$^{\Delta699/\Delta699}$ eyes show no defects. *Gli3*$^{XtJ/XtJ}$ mutant embryonic eyes show a variety of defects. Besides different degrees of microphthalmia (indicated by white arrowheads) they can display an aphakia (small/absent lens; indicated by yellow asterisk), a pigmented optic nerve (indicated by yellow arrowhead) or a coloboma (indicated by red arrowhead). The scale bar represents a length of 500 µm. (D) HE staining of eyes at embryonic stage E18.5. WT (n = 12) and *Gli3*$^{\Delta699/\Delta699}$ (n = 4) embryos show no eye defects. *Gli3*$^{XtJ/XtJ}$ embryos (n = 16) exhibit a variety of defects (100%) ranging from eye chamber defects (indicated by yellow asterisks) to anophthalmia (indicated by black arrow). In most of the cases *Gli3*$^{XtJ/XtJ}$ embryos display a microphthalmia (indicated by black arrowheads), which can be combined with other abnormalities like coloboma, a pigmented optic nerve (indicated by yellow arrowhead) or a hyaloid hyper cellularity (indicated by blue asterisk). Additional defects like a lens stalk persistence (indicated by blue arrowhead) as well as a neural retina degeneration (indicated by green asterisk), a neural retina thickening (indicated by green arrowhead) or a retinal dysplasia (indicated by green arrow) can be observed. Moreover, a total absence of the eye (anophthalmia; indicated by black arrow) with remnants of eye structures like pigmented cells (indicated by yellow arrowheads) and extraocular muscles can be monitored in *Gli3*$^{XtJ/XtJ}$ embryos. Percentages indicate the defect frequencies. The scale bar represents a length of 500 µm. C, cornea; NR, neural retina; RPE, retinal pigmented epithelium.

of every eye. In contrast to the *Gli3*$^{XtJ/XtJ}$ embryos, all examined *Gli3*$^{\Delta699/\Delta699}$ mouse embryos displayed eyes which looked completely normal (Fig. 1A–D). These findings indicate that GLI3-R contributes significantly to proper eye morphogenesis, while GLI3-A seems to play no role at all.

2.2. Key players of eye development are altered in *Gli3*$^{XtJ/XtJ}$ eyes

Our phenotypic investigations at E18.5 revealed that 100% of the *Gli3*$^{\Delta699/\Delta699}$ eyes develop normally whereas 100% of all analysed *Gli3*$^{XtJ/XtJ}$ eyes are defective. However, the effects of these mutations at the molecular level are unknown. To obtain a comprehensive view of the transcriptional consequences caused by the different mutations, we assayed gene expression of *Gli3*$^{XtJ/XtJ}$ and *Gli3*$^{\Delta699/\Delta699}$ murine eyes at E18.5. This embryonic day allowed us to obtain sufficient RNA from accurately isolated eyes of individual mouse embryos without pooling them. To ensure that enough RNA from *Gli3*$^{XtJ/XtJ}$ eyes was available, only *Gli3*$^{XtJ/XtJ}$ eyes with the mild mutant phenotype (mild microphthalmia) were used. The microarray assay revealed that in both, *Gli3*$^{\Delta699/\Delta699}$ and *Gli3*$^{XtJ/XtJ}$ eyes, numerous transcripts were differentially expressed (Fig. 2A and Tables S1–9). In this context, the individual samples of each mutant showed consistent results (Fig. 2B). Surprisingly, the number of altered gene expressions was higher in *Gli3*$^{\Delta699/\Delta699}$ eyes (1532 differentially expressed genes) than in *Gli3*$^{XtJ/XtJ}$ eyes (1095 differentially expressed genes) demonstrating that, at the molecular level, eye development is altered by both mutations. Analysing causal relationships of the altered gene expressions in the respective mutant eyes by using the Ingenuity Pathway Analysis software (IPA; Qiagen) (Krämer et al., 2014), we recognised that a large number of genes which represent key players in eye development (*Aldh1a3*, *Smoc1*, *Odz3*, *Foxe3*, *Hes1*, *Tfap2a*, *Tbx2*, *Tbx5*, *Fgf15*, *EphrinB2*, *Gja8* and *Cryab* (Andley et al., 2011; Bakthavachalu et al., 2010; Bassett et al., 2007; Behesti et al., 2006; Behesti et al., 2009; Ben-Zur et al., 2000; Blixt et al., 2000; Brownell et al., 2000; Chapman et al., 1996; Chassaing et al., 2016; Dupé et al., 2003; Kerscher et al., 1995; Koshiba-Takeuchi et al., 2000; Kurose et al., 2004; Leamey et al., 2007; Lee et al., 2005; Matt et al., 2005; Merlin et al., 2013; Mic et al., 2000; Okada et al., 2011; Rainger et al., 2011; Steele et al., 1998; Suzuki et al., 2000; Takatsuka et al., 2004; Templeton et al., 2013; Tomita et al., 1996)) showed a changed expression in *Gli3*$^{XtJ/XtJ}$ but not in *Gli3*$^{\Delta699/\Delta699}$ embryonic eyes. *Cryab*, *Gja8*, *Hes1*, *Tfap2a*, *Tbx2*, *Tbx5*, *Fgf15* and *EphrinB2* were downregulated in *Gli3*$^{XtJ/XtJ}$ eyes and unaltered in *Gli3*$^{\Delta699/\Delta699}$ eyes (Fig. 2C), while *Odz3*, *Smoc1* and *Foxn3* were upregulated in *Gli3*$^{XtJ/XtJ}$ eyes and unaltered in *Gli3*$^{\Delta699/\Delta699}$ eyes (Fig. 2C). In two cases, the expression of genes which are deeply involved in eye development was changed in both *Gli3*$^{XtJ/XtJ}$ and *Gli3*$^{\Delta699/\Delta699}$ eyes but in different directions. *Aldh1a3* was upregulated in *Gli3*$^{XtJ/XtJ}$ eyes and downregulated in *Gli3*$^{\Delta699/\Delta699}$ eyes, while *Foxe3* was downregulated in *Gli3*$^{XtJ/XtJ}$ eyes and upregulated in *Gli3*$^{\Delta699/\Delta699}$ eyes (Fig. 2C). We confirmed the microarray data by performing qRT-PCR studies for selected gene expressions (Fig. 2D–G).

Table 1
Frequencies of eye defects in WT, *Gli3*$^{XtJ/XtJ}$ and *Gli3*$^{\Delta699/\Delta699}$ embryonic eyes at embryonic stages E14.5 and E18.5.

embryonic stage	genotype	n	eye defects	frequency
E14.5	*Gli3*$^{+/+}$	21	0/21	0%
	Gli3$^{XtJ/XtJ}$	22	11/22	50%
	Gli3$^{\Delta699/\Delta699}$	14	0/14	0%
E18.5	*Gli3*$^{+/+}$	12	0/12	0%
	Gli3$^{XtJ/XtJ}$	16	16/16	100%
	Gli3$^{\Delta699/\Delta699}$	4	0/4	0%
E14.5 + E18.5	*Gli3*$^{+/+}$	33	0/33	0%
	Gli3$^{XtJ/XtJ}$	38	27/38	71%
	Gli3$^{\Delta699/\Delta699}$	18	0/18	0%

2.3. GLI3-R regulates proliferation of the eye at late developmental stages

Several genes (*Foxe3*, *Hes1*, *Tbx2*, *Fgf15*, *Gja8*) whose expression was downregulated in *Gli3*$^{XtJ/XtJ}$ eyes and that play important roles in eye development are known to be positive regulators of cell proliferation during eye formation (Behesti et al., 2009; Medina-Martinez et al., 2005; Wall et al., 2009; Wang et al., 2016, 2017). Interestingly, the expression of these genes was upregulated (*Foxe3*) or not changed at all (*Hes1*, *Tbx2*, *Fgf15*, *Gja8*) in *Gli3*$^{\Delta699/\Delta699}$ eyes (Fig. 2C). Since cell proliferation is indispensable for proper vertebrate eye development (Bozanić and Saraga-Babić, 2004; Fuhrmann, 2010), we investigated proliferation in mouse embryonic eyes at E18.5. Again, we used *Gli3*$^{XtJ/XtJ}$ eyes which exhibit a mild microphthalmia. In comparison to wild-type eyes, the proliferation rate was unaltered in *Gli3*$^{\Delta699/\Delta699}$ eyes, while it was reduced in the absence of GLI3 (Fig. 3A). To elucidate whether the changes in these cellular processes also exist in earlier stages of eye development in *Gli3*$^{XtJ/XtJ}$ mouse embryos, we quantified the proliferation rate at E12.5. The proliferation rate was unaltered in both *Gli3*$^{XtJ/XtJ}$ and *Gli3*$^{\Delta699/\Delta699}$ eyes in comparison to wild-type eyes at E12.5 (Fig. 3B). Consequently, the defects which were observed in *Gli3*$^{XtJ/XtJ}$ eyes at E14.5 are not caused by a reduced proliferation rate. Nevertheless, it can be assumed that the GLI3-R has an influence on eye development at later developmental stages by at least the control of proliferation (Fig. 3A).

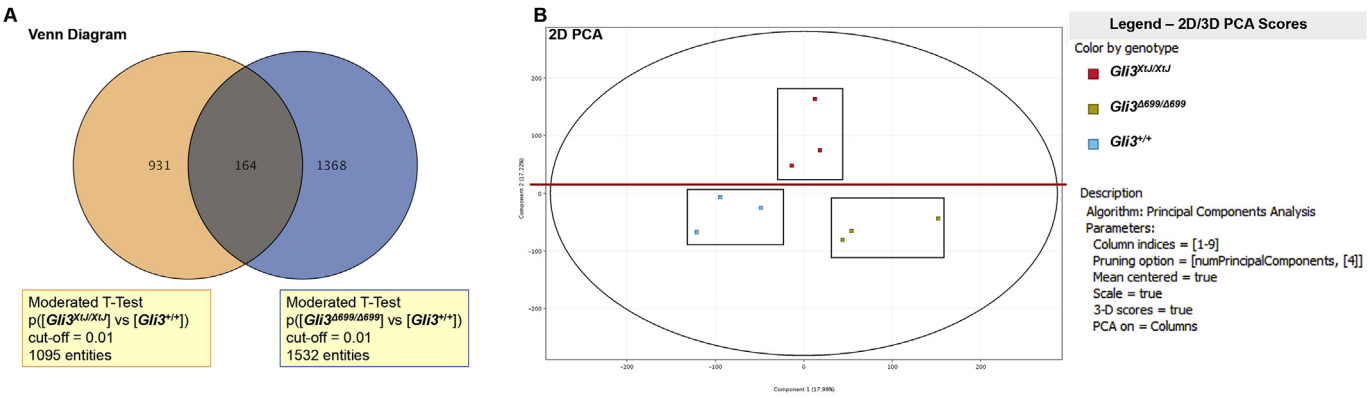

C

gene	$Gli3^{Xt/Xt}$	$Gli3^{\Delta699/\Delta699}$	expression	function	mutant phenotype	references
Aldh1a3	↑	↓	surface ectoderm, dorsal RPE, ventral NR	invagination of optic cup, cornea and eyelid morphogenesis (apoptosis in perioptic mesenchyme), RA-synthesis	disease gene for non-syndromic microphthalmia in humans; shortening of ventral retina, incomplete closure of the choroid fissure	Dupé et al., 2003; Matt et al., 2005; Mic et al., 2000; Suzuki et al., 2000
Smoc1	↑	→	optic stalk, optic cup	ocular and limb development, Bmp-antagonist	iris and retinal defects (colobomas), small eyes, defects of optic nerve, retina and RPE	Okada et al., 2011; Rainger et al., 2011
Odz3	↑	→	retina, optic stalk, lens	Axonal guidance	microphthalmia	Ben-Zur et al., 2000; Chassaing et al., 2016; Leamey et al., 2007; Merlin et al., 2013
Foxe3	↓	↑	lens placode, lens vesicle, lens epithelium	lens placode formation, fiber cell differentiation	variable; lens defects, reduced anterior eye chamber, increased cell death	Blixt et al., 2000; Brownellet al., 2000
Hes1	↓	→	optic vesicle, optic cup, forming lens, epithelial cells, RPE	essential for growth, morphogenesis, differentiation, retinal neurogenesis	variable; small and deformed optic cups with ventral opening, lack of neural retina, remnant of pigmented epithelium, defects of lens and cornea	Lee et al., 20051; Takatsuka et al., 2004; Tomita et al., 1996
Tfap2a	↓	→	retina	crucial regulator of ocular morphogenesis especially of the retina	defects in developing optic cup, neural retina patterning, replacement of RPE by stalk and retina	Bassett et al., 2007
Tbx2	↓	→	presumptive retina during optic vesicle invagination	optic cup formation, cell cycle regulation, tissue growth and development along the DV axis, important for maintenance of *Tbx5*-expression	delayed ventral optic vesicle invagination, small and abnormally shaped optic cups, reduced retinal volume (increased apoptosis), reduced *Tbx5*- and *Fgf15*-expression	Behesti et al., 2006; Behesti et al., 2009
Tbx5	↓	→	dorsal retina	key determinant for dorsal retina development (DV patterning)		Behesti et al., 2006; Chapman et al., 1996; Koshiba-Takeuchi et al., 2000
Fgf15	↓	→	retina (NR versus RPE)	proliferation marker		Behesti et al., 2009; Kurose et al., 2004
EphrinB2	↓	→	dorsal retina	topographic guidance molecule	failure of optic nerve formation	Behesti et al., 2009
Gja8	↓	→	lens fibre	gap junction channel	cataract, mircrophthalmia	Bakthavachalu et al., 2010; Kerscher et al., 1995; Steele et al., 1998
Cryab	↓	→	lens, retina			Andley et al., 2011; Templeton et al., 2013

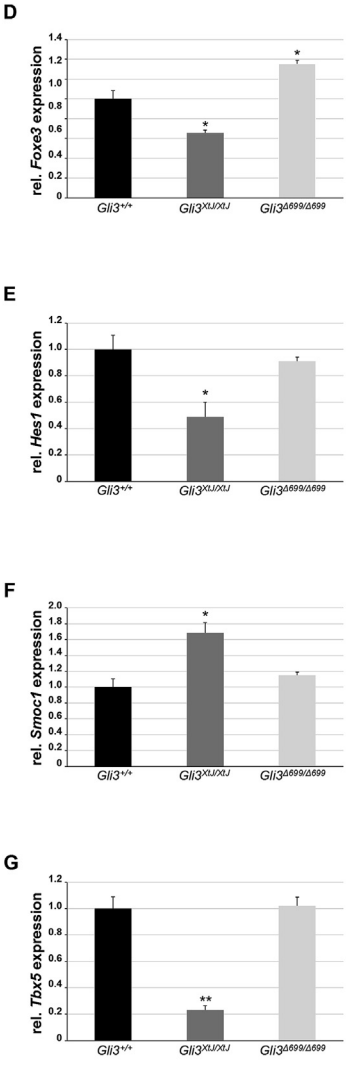

Fig. 2. Genes which are known to play crucial roles in eye development are differentially expressed in the eyes of $Gli3^{XtJ/XtJ}$ mutant embryos at E18.5. (A–C) Microarray assay was performed using RNA isolates from WT (n = 3), $Gli3^{XtJ/XtJ}$ (n = 3) and $Gli3^{\Delta699/\Delta699}$ (n = 3) eyes at embryonic stage E18.5. (A) Venn diagram shows differentially expressed genes in $Gli3^{XtJ/XtJ}$ (red circle) and in $Gli3^{\Delta699/\Delta699}$ (blue circle) eyes compared to WT eyes. A fold change of minimum 1.5 was defined for differentially expressed genes. (B) 2D Principle Components Analysis (PCA) illustrates a distinct clustering of the WT, $Gli3^{XtJ/XtJ}$ and $Gli3^{\Delta699/\Delta699}$ values. Black squares indicate the grouped genotypes. The red line denotes the difference between $Gli3^{XtJ/XtJ}$ (above zero) and WT and $Gli3^{\Delta699/\Delta699}$ (below zero). (C) List of genes which play crucial roles in eye development and their change of expression in $Gli3^{XtJ/XtJ}$ and $Gli3^{\Delta699/\Delta699}$ eyes. (D–G) Confirmation of Microarray assay results for *Foxe3* (D), *Hes1* (E), *Smoc1* (F) and *Tbx5* (G) via qRT-PCR analyses. Lysates were obtained from WT (D: n = 3; E: n = 5; F: n = 4; G: n = 3), $Gli3^{XtJ/XtJ}$ mutant (D: n = 5; E: n = 4, F: n = 3; G: n = 3) and $Gli3^{\Delta699/\Delta699}$ mutant (D: n = 3; E: n = 4; F: n = 3; G: = 3) embryonic eyes. The WT bars were normalised to 1. Data are shown as mean ± s.e.m. Asterisks denote statistical significance according to one-way ANOVA and Tukey HSD tests (*P < 0.05; **P < 0.01) (D: $F(2, 8) = 11.69$, P < 0.0042; E: $F(2, 10) = 6.455$, P < 0.0158; F: $F(2, 7) = 8.828$, P < 0.0122; G: $F(2, 6) = 23.53$, P < 0.0014).

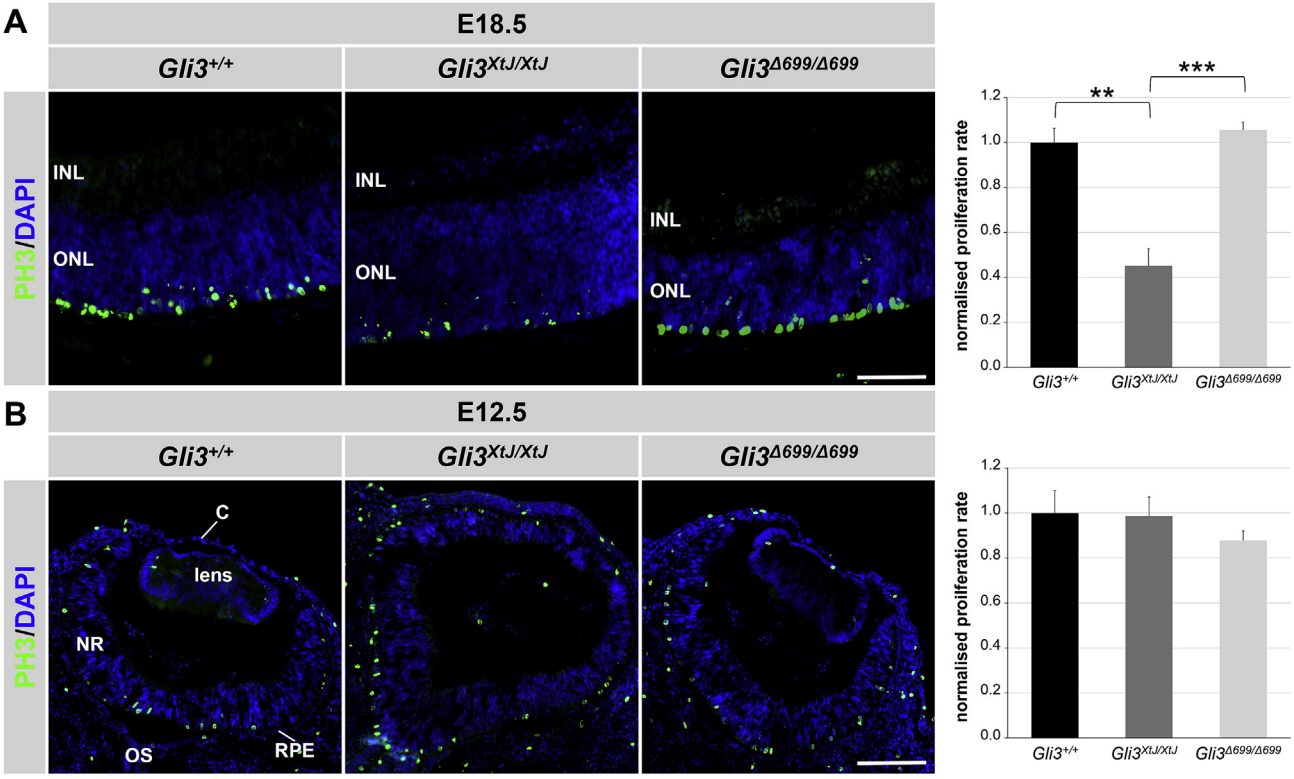

Fig. 3. *Gli3*$^{XtJ/XtJ}$ mutant mouse embryos show a reduced proliferation rate in the eyes at E18.5 but not at E12.5. (A, B) Immunofluorescence on mouse embryonic eyes at embryonic stages (A) E18.5 and (B) E12.5. Cryosections were obtained from WT, *Gli3*$^{XtJ/XtJ}$ and *Gli3*$^{\Delta699/\Delta699}$ mouse embryos and stained with DAPI (in blue) and anti-phospho Histone H3 (pH3 in green). At least 6 sections per individual were used for quantification. The number of pH3-positive cells in the eyes were counted and related to the total cell number. Finally, the proliferation rates were normalised to WT. The scale bars in white represent a length of 200 µm. Data are shown as mean ± s.e.m. Asterisks denote statistical significance according to one-way ANOVA and Tukey HSD tests (***$P < 0.001$) (A: F (2, 29) = 11.5, $P < 0.0002$). (A) The quantification of pH3-positive cells per eye shows a significant decreased proliferation rate in eyes of *Gli3*$^{XtJ/XtJ}$ mutant mouse embryos at embryonic stage E18.5. Eyes of *Gli3*$^{\Delta699/\Delta699}$ mutants display no alteration in the proliferation rate (WT: n = 3; *Gli3*$^{XtJ/XtJ}$: n = 3; *Gli3*$^{\Delta699/\Delta699}$: n = 3). INL, inner nuclear layer; ONL, outer nuclear layer. (B) Quantification of pH3-positive cells per eye show no differences in proliferation rates between WT, *Gli3*$^{XtJ/XtJ}$ and *Gli3*$^{\Delta699/\Delta699}$ mutants at embryonic stage E12.5 (WT: n = 5; *Gli3*$^{XtJ/XtJ}$: n = 5; *Gli3*$^{\Delta699/\Delta699}$: n = 5). C, cornea; NR, neural retina; ON, optic nerve; RPE, retinal pigmented epithelium.

2.4. GLI3-R regulates pattern formation of several genes and proteins involved in early eye development

In search of the molecular differences between *Gli3*$^{XtJ/XtJ}$ and *Gli3*$^{\Delta699/\Delta699}$ eyes at E12.5, we analysed the expression pattern of genes which are known to be essential for eye development at this time by performing in situ hybridisation studies. The expression pattern of *Pax6* was unaltered in the eyes of both mutants (Fig. 4A). *Pax2* expression pattern was expanded from the optic nerve to the neural retina in *Gli3*$^{XtJ/XtJ}$ eyes, while it was unaltered in *Gli3*$^{\Delta699/\Delta699}$ eyes (Fig. 4A). Thus, the expression of *Pax2* was increased in the absence of GLI3 but unchanged in the presence of GLI3-R alone. These results were confirmed by qRT-PCR studies (Fig. 4B). The expression pattern of *Six3* and *Vax2* were decreased in *Gli3*$^{XtJ/XtJ}$ eyes and unaltered in *Gli3*$^{\Delta699/\Delta699}$ eyes (Fig. 4A). In the case of *Six3*, the result was confirmed by a qRT-PCR study (Fig. 4C). *Wnt3a* expression pattern was increased in *Gli3*$^{XtJ/XtJ}$ eyes and unchanged in *Gli3*$^{\Delta699/\Delta699}$ eyes (Fig. 4A). To get a deeper insight into eye patterning of *Gli3*$^{XtJ/XtJ}$ and *Gli3*$^{\Delta699/\Delta699}$ eyes, we analysed additional factors by performing immunofluorescence studies. We detected an expansion of OTX2, PAX2 and SOX1 into the neural retina of *Gli3*$^{XtJ/XtJ}$ eyes, while the localisation of these proteins was unchanged in *Gli3*$^{\Delta699/\Delta699}$ eyes (Fig. 5A–C). In the case of PAX2, these data confirm the results of the in situ hybridisation study (Fig. 4A). While the expression pattern of SOX2 was reduced in *Gli3*$^{XtJ/XtJ}$ eyes, it was properly localised in *Gli3*$^{\Delta699/\Delta699}$ eyes (Fig. 5D).

2.5. GLI3-R influences canonical WNT-signalling in early stages of eye development

In a former study, we suggested that GLI3 realises its effect on eye development via DKK1 (Lieven and Rüther, 2011). To get an idea of whether our hypothesis might be true, we performed immunofluorescence studies for DKK1 in *Gli3*$^{XtJ/XtJ}$ and *Gli3*$^{\Delta699/\Delta699}$ eyes. The expression pattern of DKK1 was decreased in the lens and the optic stalk of *Gli3*$^{XtJ/XtJ}$ eyes and unaltered in *Gli3*$^{\Delta699/\Delta699}$eyes (Fig. 6A). This finding was confirmed by a qRT-PCR analysis (Fig. S1). In a former study, we elucidated that MSX2 directly binds to the conserved non-coding element (CNE)195 optic cup enhancer of *Dkk1* (Lieven et al., 2014). Interestingly, *Msx2* is a target of GLI3-R (Lallemand et al., 2009) and MSX2 functions as a transcriptional repressor (Semenza et al., 1995). All these findings are in line with our hypothesis that GLI3-R might regulate the expression of *Dkk1* via controlling *Msx2*. To get further insights in the relation between *Gli3-R*, *Dkk1* and *Msx2*, we examined MSX2 in *Gli3*$^{XtJ/XtJ}$ and *Gli3*$^{\Delta699/\Delta699}$ eyes. The expression pattern of MSX2 was unchanged in the eyes of both mutants (Fig. 6B). Since DKK1 is an antagonist of WNT/β-CATENIN signalling (Fedi et al., 1999; Glinka et al., 1998), we analysed β-CATENIN in *Gli3*$^{XtJ/XtJ}$ and *Gli3*$^{\Delta699/\Delta699}$ eyes. Due to the fact that many antibodies are not suitable for immunofluorescence studies on eye tissue, we firstly tested several antibodies for their eligibility. The illustrated immunofluorescence staining provided a nuclear signal that is characteristic for β-CATENIN in active canonical WNT signalling (Fig. S2). Thus, the staining allowed us to perform comparative examinations. While we detected no difference between wild-type and

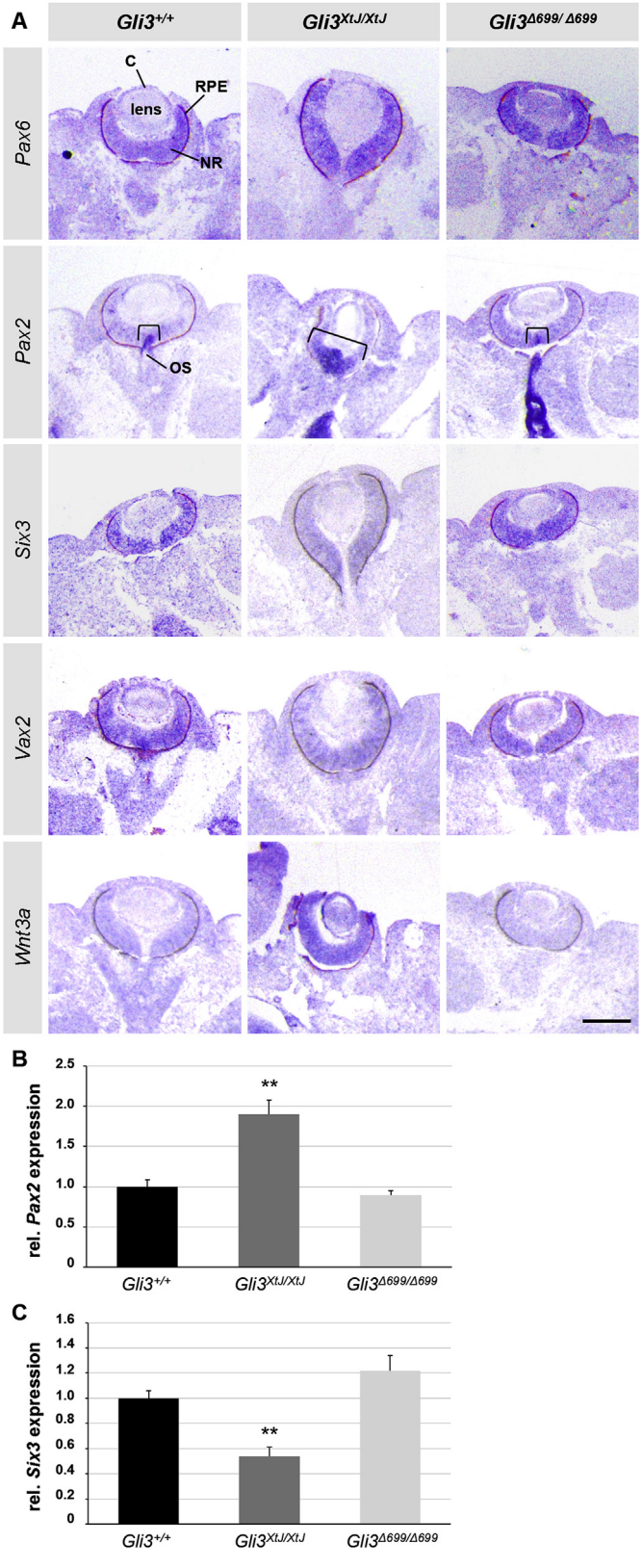

(caption on next column)

Fig. 4. Unaltered gene expression patterns in *Gli3*$^{\Delta 699/\Delta 699}$ mutant mouse embryonic eyes at E12.5, while the expression pattern of several key players in eye formation are changed in E12.5 *Gli3*$^{XtJ/XtJ}$ eyes. (A) *In situ* hybridisation on transversal sections of WT, *Gli3*$^{\Delta 699/\Delta 699}$ and *Gli3*$^{XtJ/XtJ}$ eyes at embryonic stage E12.5. The expression pattern of *Pax6* is unaltered in *Gli3*$^{\Delta 699/\Delta 699}$ and *Gli3*$^{XtJ/XtJ}$ mutant embryonic eyes. The expression pattern of *Pax2* is expanded from the optic nerve to the neural retina in *Gli3*$^{XtJ/XtJ}$ mutants and unaltered in eyes of *Gli3*$^{\Delta 699/\Delta 699}$ embryos (indicated by black brackets). *Six3* and *Vax2* expression patterns are weaker in the eyes of *Gli3*$^{XtJ/XtJ}$ mutants and unaltered in eyes of *Gli3*$^{\Delta 699/\Delta 699}$ mutants. The expression pattern of *Wnt3a* is increased in *Gli3*$^{XtJ/XtJ}$ mutant eyes and unaltered in eyes of *Gli3*$^{\Delta 699/\Delta 699}$ mutants. The scale bar represents a length of 250 µm. C, cornea; NR, neural retina; ON, optic nerve; RPE, retinal pigmented epithelium. (B, C) Confirmation of in situ hybridisation results for *Pax2* (B) and *Six3* (C) via qRT-PCR analyses. Lysates were obtained from WT (B: n = 3; C: n = 5), *Gli3*$^{XtJ/XtJ}$ mutant (B: n = 3; C: n = 4) and *Gli3*$^{\Delta 699/\Delta 699}$ mutant (B: n = 3; C: n = 3) embryonic eyes. The WT bars were normalised to 1. Data are shown as mean ± s.e.m. Asterisks denote statistical significance according to one-way ANOVA and Tukey HSD tests (**$P < 0.01$) (B: F (2, 6) = 15.64, $P < 0.0042$; C: F (2, 9) = 13.34, $P < 0.002$).

Gli3$^{\Delta 699/\Delta 699}$ eyes regarding the localisation of β-CATENIN, its expression pattern was strongly increased in *Gli3*$^{XtJ/XtJ}$ eyes (Fig. 6C). In summary, our data reveal that GLI3-A is dispensable for vertebrate eye morphogenesis and that GLI3-R regulates eye formation by ensuring proper expression pattern of well-known key players in eye development.

3. Discussion

The transcription factor GLI3 mediates the transduction of HH signalling and is essential for the development of numerous structures and organs in vertebrates. Considering that GLI3 is expressed in the eye and that *Gli3*$^{XtJ/XtJ}$ mouse embryos which lack GLI3 display severe eye defects (Choi et al., 2014; Franz and Besecke, 1991; Johnson, 1967), it is obvious that GLI3 plays a pivotal role in eye development. However, it was reported that some *Gli3*$^{XtJ/XtJ}$ embryos form “apparently normal” eyes at E11.5 (Franz and Besecke, 1991). We detected several eye defects (microphthalmia, anophthalmia, lens stalk persistence, hyaloid hypercellularity, defects in the formation of the anterior and posterior eye chamber, loss of several eye structures etc.) in 71% of all analysed *Gli3*$^{XtJ/XtJ}$ embryos (Table 1). The frequency of 71% suggests that GLI3 is not necessary for the development of every eye but a closer look on the defect statistics contradicts this suggestion. While 50% of the analysed *Gli3*$^{XtJ/XtJ}$ embryos displayed eye abnormalities at E14.5, 100% of these embryos exhibited eye defects at E18.5 (Table 1) demonstrating that GLI3 deficiency also affects eye development after E14.5. Consequently, GLI3 is absolutely essential for eye morphogenesis. In dependency of the presence or absence of the HH ligand, GLI3 functions either as a transcriptional activator or as a transcriptional repressor (Sasaki et al., 1999; Wang et al., 2000). Previous studies showed that GLI3 deficiency alters the expression of genes which are essential for eye development (Aoto et al., 2002; Furimsky and Wallace, 2006; Zaki et al., 2006). However, these studies did not allow to distinguish between GLI3-A and GLI3-R, since they were performed by using *Gli3*$^{XtJ/XtJ}$ mouse embryos which lack both GLI3-A and GLI3-R. In our current study, we used *Gli3*$^{XtJ/XtJ}$ and *Gli3*$^{\Delta 699/\Delta 699}$ embryos. In *Gli3*$^{\Delta 699/\Delta 699}$ embryos, GLI3-R is constitutively active, while GLI3-A is missing (Böse et al., 2002). Thus, the comparison of the two mouse mutants provides insights into the specific functions of GLI3-A and GLI3-R. Importantly, we observed no eye defects in *Gli3*$^{\Delta 699/\Delta 699}$ embryos (Fig. 1 and Table 1). In combination with the fact that the absence of GLI3 leads to eye defects in 100% of all analysed eyes at E18.5 (Table 1), these data show that GLI3-A is dispensable in eye morphogenesis, while GLI3-R is essential for eye development. Remarkably, it was previously reported that GLI3$^{\Delta 699}$ may not be as potent as the natural occurring GLI3-R (Cao et al., 2013). Since *Gli3*$^{\Delta 699/\Delta 699}$ embryos display no obvious morphological eye defects, even a small amount of GLI3-R might be sufficient to ensure proper eye development. Investigations in mouse mutants which suffer from a ciliary

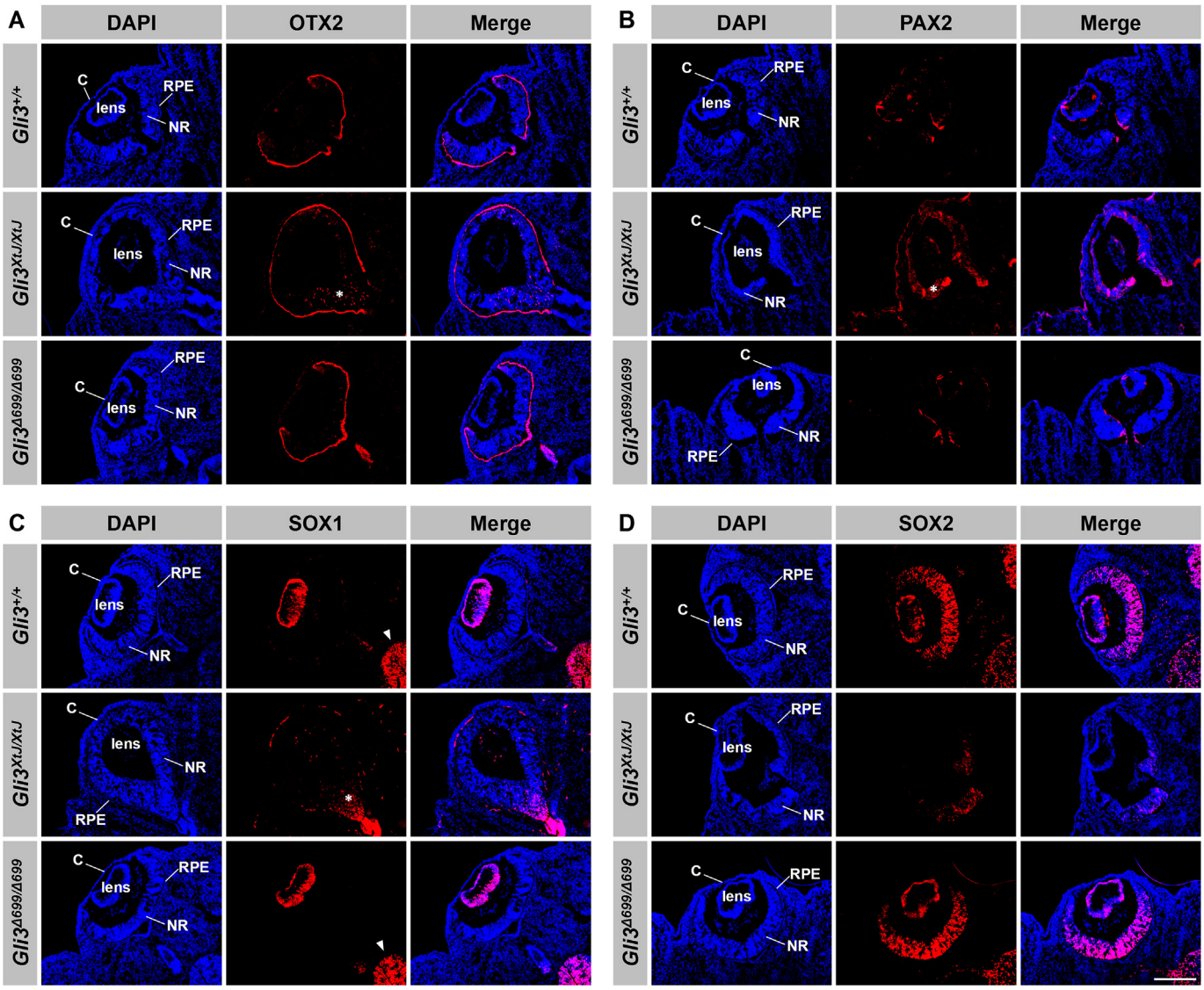

Fig. 5. Unaltered localisation of proteins associated to eye formation in *Gli3*$^{\Delta 699/\Delta 699}$ mutant mouse embryonic eyes at E12.5, while the localisation of these proteins is changed in E12.5 *Gli3*$^{XtJ/XtJ}$ eyes. (A–D) Immunofluorescence on mouse embryonic eyes at embryonic stage E12.5. Cryosections were obtained from WT (n = 5), *Gli3*$^{XtJ/XtJ}$ (n = 5) and *Gli3*$^{\Delta 699/\Delta 699}$ (n = 5) mouse embryos. The scale bars in white represent a length of 200 μm. C, cornea; NR, neural retina; RPE, retinal pigmented epithelium. (A) OTX2 is detectable in the retinal pigmented epithelium of WT and *Gli3*$^{\Delta 699/\Delta 699}$ embryonic eyes. In eyes of *Gli3*$^{XtJ/XtJ}$ mutants OTX2 expands from the retinal pigmented epithelium to the neural retina (indicated by a white asterisk). (B) PAX2 is restricted to the optic nerve in WT and *Gli3*$^{\Delta 699/\Delta 699}$ embryonic eyes and expanded in the neural retina of *Gli3*$^{XtJ/XtJ}$ mutants (indicated by a white asterisk). (C) The marker SOX1 is detectable in the lenses of WT and *Gli3*$^{\Delta 699/\Delta 699}$ embryos as well as neuronal tissue (indicated by white arrowheads). In eyes of *Gli3*$^{XtJ/XtJ}$ mutants SOX1 is distally expanded in the neural retina (indicated by a white asterisk). (D) SOX2 is expressed in the neural retina of WT and *Gli3*$^{\Delta 699/\Delta 699}$ embryos and a weaker expression pattern is detectable in *Gli3*$^{XtJ/XtJ}$ mutant eyes.

dysfunction revealed that primary cilia ensure proper murine eye formation by controlling the amount of GLI3-R (Burnett et al., 2017). This finding is supported by a study that examined ocular development in *Rpgrip1l*$^{-/-}$ embryos which suffer from a ciliary dysfunction (Andreu-Cervera et al., 2019). RPGRIP1L is a ciliary protein whose loss results in ciliary dysfunction, in turn leading to an impaired transduction of several signalling pathways, reduced autophagy and a decreased activity of the cilia-regulated proteasome in vertebrates (Chen et al., 2015; Gerhardt et al., 2013, 2015, 2016a; Mahuzier et al., 2012; Struchtrup et al., 2018; Vierkotten et al., 2007; Wiegering et al., 2017, 2018a). Importantly, RPGRIP1L deficiency results in a reduced amount of GLI3-R (Besse et al., 2011; Gerhardt et al., 2013, 2015, 2016b; Vierkotten et al., 2007; Wiegering et al., 2018b). Previously, it was shown that *Rpgrip1l*$^{-/-}$ embryos display microphthalmia, deep set or even no detectable eyes (Delous et al., 2007; Vierkotten et al., 2007). The frequency of eye defects in these embryos is about 80% (Wiegering et al., 2018a). Andreu-Cervera and colleagues revealed that the introduction of the *Gli3*$^{\Delta 699}$ allele into *Rpgrip1l*-negative embryos results in a partial rescue of early eye development (Andreu-Cervera et al., 2019). The outcome of this experiment highlights the important role of GLI3-R in eye development.

Although the morphology of the *Gli3*$^{\Delta 699/\Delta 699}$ eyes was not different from wild-type eyes, the gene expression profile at E18.5 differed tremendously (Fig. 2A and B). 1532 genes were differentially expressed (Fig. 2A). Apart from the eye, *Gli3*$^{\Delta 699/\Delta 699}$ mouse embryos exhibited massive developmental disorders which result in perinatal death. They suffer from malformations of the respiratory system, an imperforate anus, genital abnormalities, intestinal defects, the absence of the epiglottis, a laryngeal cleft, the loss of the adrenal gland, the absence of one kidney combined with phenotypic abnormalities in the remaining kidney, bone and skull malformations and a proximo-distal shortening of the limbs,

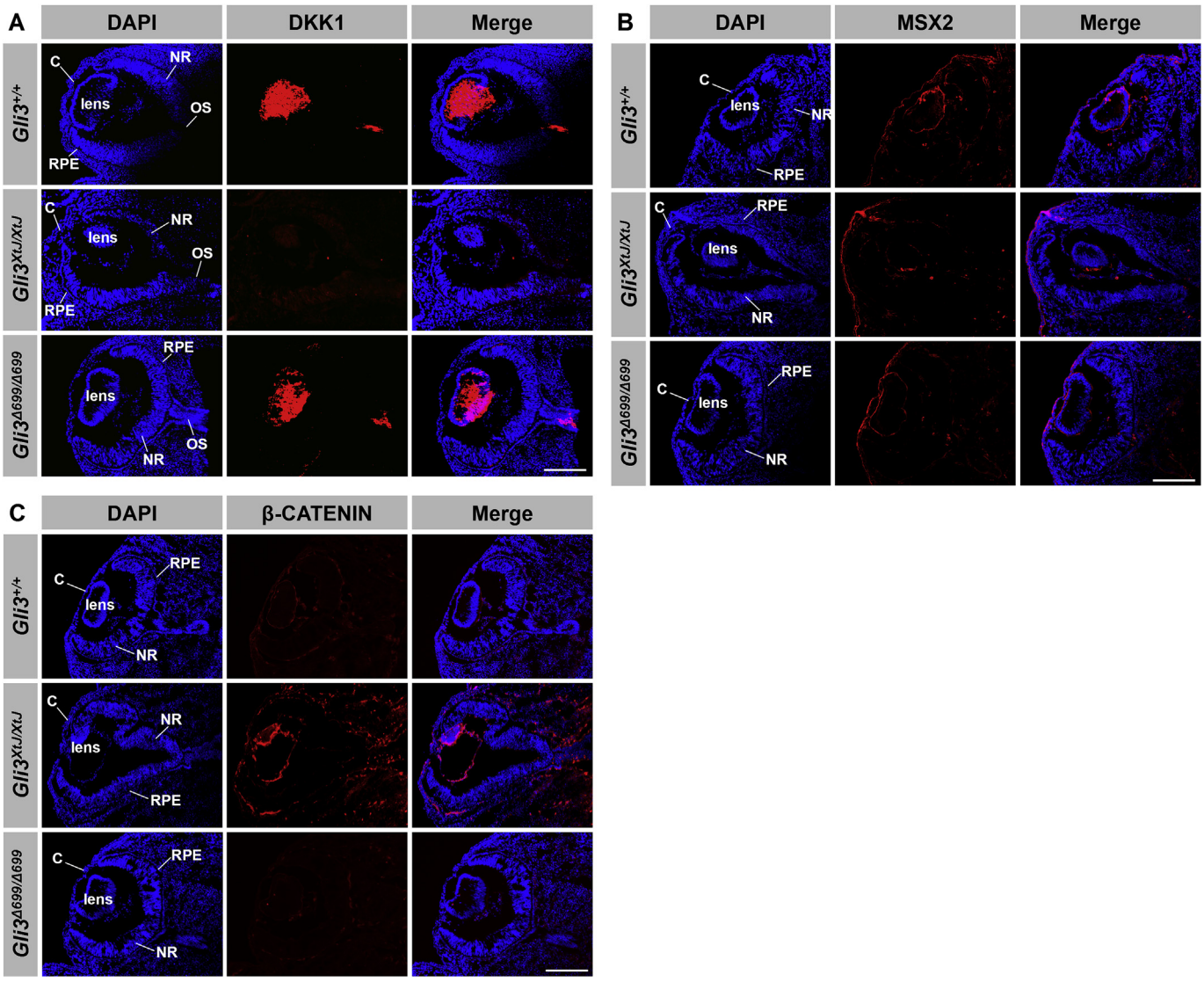

Fig. 6. Unaltered localisation of proteins associated to WNT signalling in *Gli3*$^{\Delta 699/\Delta 699}$ mutant mouse embryonic eyes at E12.5, while the localisation of these proteins is changed in E12.5 *Gli3*$^{XtJ/XtJ}$ eyes. (A–C) Immunofluorescence on mouse embryonic eyes at embryonic stage E12.5. Cryosections (A–C) were obtained from WT (n = 5), *Gli3*$^{XtJ/XtJ}$ (n = 5) and *Gli3*$^{\Delta 699/\Delta 699}$ (n = 5) mouse embryos. The scale bars in white represent a length of 200 μm. C, cornea; NR, neural retina; RPE, retinal pigmented epithelium. (A) DKK1 is detectable in the lens and optic stalk of WT and *Gli3*$^{\Delta 699/\Delta 699}$ embryonic eyes. The DKK1 pattern in eyes of *Gli3*$^{XtJ/XtJ}$ mutants is reduced. (B) MSX2 is located in the retina, the cornea and the lens and is unaltered in *Gli3*$^{\Delta 699/\Delta 699}$ and *Gli3*$^{XtJ/XtJ}$ eyes. (C) A low amount of β-CATENIN is detectable in the lens, the RPE and the hyaloid canal of WT and *Gli3*$^{\Delta 699/\Delta 699}$ eyes. In eyes of *Gli3*$^{XtJ/XtJ}$ mutants β-CATENIN shows an increased expression pattern in the lens and optic stalk.

syndactyly and polydactyly (Böse et al., 2002; Cao et al., 2013; He et al., 2016; Hill et al., 2009). Importantly, the eye tolerates the radically altered genetics and belongs to the few organs which do not show external abnormalities. This is very remarkable, especially in the context of the finding that the microphthalmic *Gli3*$^{XtJ/XtJ}$ eyes evinced only 1095 differentially expressed genes (Fig. 2A). Interestingly, both mutants share only 164 differentially expressed genes (Fig. 2A). However, there were several among the differentially expressed genes in *Gli3*$^{XtJ/XtJ}$ eyes which are known to be pivotal for eye development. The expression of most of these genes (e.g. *Cryab, Gja8*, *Hes1*, *Tfap2a*, *Tbx2*, *Tbx5*, *Fgf15*, *EphrinB2*, *Odz3*, *Rab23*, *Smoc1* and *Foxn3*) was unaltered in *Gli3*$^{\Delta 699/\Delta 699}$ eyes (Fig. 2C). The minority of these genes (e.g. *Aldh1a3* and *Foxe3*) was changed in opposing directions in the eyes of the two different mutants (Fig. 2C). Consequently, GLI3-R controls the genetic program which is needed for proper eye formation. One central process in eye development is proliferation (Bozanić and Saraga-Babić, 2004; Fuhrmann, 2010) and many genes that show an altered expression in *Gli3*$^{XtJ/XtJ}$ eyes at E18.5 are involved in proliferation during eye development. At E18.5, the number of proliferating cells is significantly decreased in *Gli3*$^{XtJ/XtJ}$ eyes, while it is unaltered in *Gli3*$^{\Delta 699/\Delta 699}$ eyes (Fig. 3A). Since the proliferation rate in the eyes of both mutants was unchanged at E12.5 (Fig. 3B), we assumed that most of the defects in *Gli3*$^{XtJ/XtJ}$ eyes are caused by the alteration of factors that do not control proliferation. In search of the molecular mechanisms underlying the regulation of eye development by GLI3-R, we investigated the gene and/or protein expression pattern of key factors in eye development at E12.5. Our investigations revealed that GLI3-R controls the closure of the optic fissure. To test whether optic stalk patterning might be affected by the loss of GLI3-R, we compared the expression pattern of *Pax2* and PAX2 in the optic stalk of *Gli3*$^{XtJ/XtJ}$ and *Gli3*$^{\Delta 699/\Delta 699}$ eyes. We detected an expansion of its expression/localisation from the optic stalk to the neural retina in *Gli3*$^{XtJ/XtJ}$ eyes, while its expression/localisation was unchanged in *Gli3*$^{\Delta 699/\Delta 699}$ eyes at E12.5 (Figs. 4A and 5B). Considering these data, GLI3-R restricts the expression/localisation of *Pax2*/PAX2 to the optic stalk at E12.5 (Fig. 7).

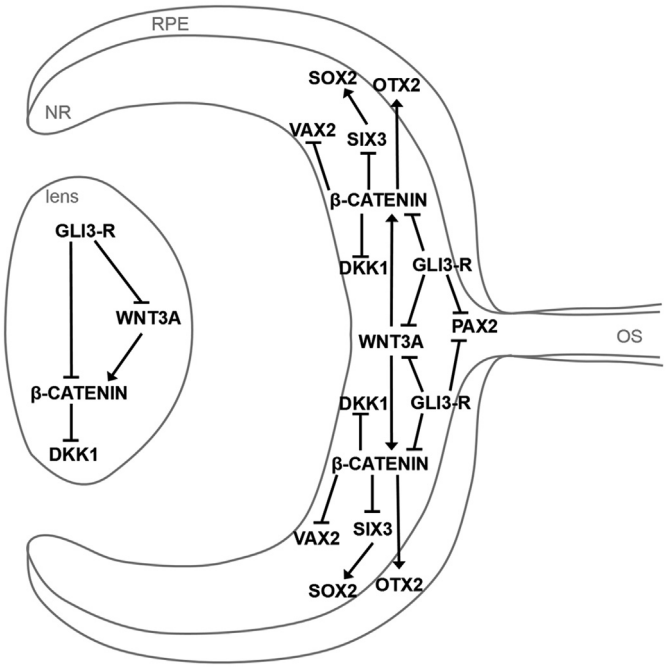

Fig. 7. Schematic model of how GLI3-R controls eye development at E12.5. We hypothesise that GLI3-R regulates WNT/β-CATENIN signalling by governing the amount of β-CATENIN in the lens and the retinal pigmented epithelium (RPE) as well as of WNT3A in the lens and in the neural retina (NR). By controlling this pathway, GLI3-R governs the amount of OTX2 in the RPE, the amount of VAX2 and SIX3 in the NR and the amount of DKK1 in the lens and the optic stalk (OS). In turn, SIX3 regulates the amount of SOX2 in the NR. Moreover, GLI3-R controls the amount of PAX2 in the OS.

Remarkably, it was formerly published that an impaired HH signalling leads to the occurrence of optic nerve defects and that HH signalling is required for the differentiation of optic disc and stalk neuroepithelial cells (Dakubo et al., 2003; Kahn et al., 2017; Take-uchi et al., 2003). Accordingly, it was shown that HH signalling promotes the expression of *Pax2* in the optic stalk at E12 in the mouse (Dakubo et al., 2003). Thus, we suggest that the repression of HH signalling by the action of GLI3-R ensures proper optic fissure closure. The boundary between optic stalk and the optic cup is established by a reciprocal inhibition between PAX2 and PAX6 (Schwarz et al., 2000). Since we detected an expansion of *Pax2* and PAX2 from the optic stalk to the neural retina in $Gli3^{XtJ/XtJ}$ eyes but not in $Gli3^{\Delta 699/\Delta 699}$ eyes (Figs. 4A and 5B), we examined the expression pattern of *Pax6* in the eyes of both mutants. Neither in $Gli3^{\Delta 699/\Delta 699}$ nor in $Gli3^{XtJ/XtJ}$ eyes, we observed an alteration of the *Pax6* expression pattern at E12.5 (Fig. 4A) demonstrating that GLI3 is not involved in governing *Pax6* expression at this time. Furthermore, we hypothesise that GLI3-R controls eye development inside a complex network of signalling cascades which are involved in eye morphogenesis at E12.5 in a great extent via regulating WNT/β-CATENIN signalling (Fig. 7). In the absence of GLI3, the expression pattern of the WNT ligand *Wnt3a* was increased in the lens and the neural retina (Fig. 4A), the expression pattern of the WNT inhibitor DKK1 was reduced in the lens and the optic stalk (Fig. 6A) and the expression pattern of the WNT signalling mediator β-CATENIN was elevated in the lens and the optic stalk (Fig. 6C). Remarkably, an enhanced amount of β-CATENIN results in the loss of lens and retinal structures as well as to a disruption of RPE patterning (Fu et al., 2006; Fujimura et al., 2009; Kreslova et al., 2007; Miller et al., 2006; Smith et al., 2005). Since it was already reported that the expression of the transcription factors *Six3*, *Vax2*, *Otx2* and *Sox2* are regulated by WNT/β-CATENIN signalling (Hägglund et al., 2013), we hypothesise that the upregulation of WNT/β-CATENIN signalling leads to the observed reduced expression of *Six3* and *Vax2* in the lens and the neural retina (Fig. 4A) as well as to the increased amount of OTX2 in the neural retina (Fig. 5A) and to the decreased amount of SOX2 in the neural retina (Fig. 5D). The alteration of these factors provoke defects in retina and lens development (Barbieri et al., 2002; Kamachi et al., 1998; Liu et al., 2006; Nishihara et al., 2012). Accordingly, SOX1 which is required for proper lens development (Kamachi et al., 1998; Nishiguchi et al., 1998) was expanded from the lens to the neural retina (Fig. 5C). In the presence of GLI3-R alone, the expression pattern of *Wnt3a*, *Six3* and *Vax2* as well as of DKK1, OTX2 and SOX2 were unaltered (Figs. 4A and 5A and D and Fig. 6A) highlighting the importance of GLI3-R for proper WNT/β-CATENIN signalling in eye development. How does GLI3-R control WNT/β-CATENIN signalling in eye morphogenesis? Our data elucidate an influence of GLI3-R on the WNT ligand WNT3A and on the WNT antagonist DKK1. It is already known that *Wnt3* contains a GLI binding site (McNeill et al., 2012). Considering that the absence of GLI3-R caused an increased expression pattern of *Wnt3a* in the lens and the neural retina (Fig. 4A), a direct transcriptional regulation of *Wnt3a* by GLI3-R is very likely. Due to the existence of several GLI3 binding sites in relevant conserved *Dkk1* regulatory sequences, we previously suggested that GLI3-R controls eye development via DKK1 (Lieven and Rüther, 2011). However, the finding that GLI3-R deficiency results in less DKK1 (Fig. 6A) argues against a direct regulation of the ocular *Dkk1* expression by GLI3-R. Furthermore, the hypothesis that GLI3-R governs the amount of DKK1 via regulating MSX2 has to be rejected. Although the transcriptional repressor MSX2 directly binds to the CNE195 optic cup enhancer of *Dkk1* (Lieven et al., 2014), *Msx2* is a target of GLI3-R (Lallemand et al., 2009) and an increased amount of MSX2 leads to congenital eye defects in mice and humans (Plaisancié et al., 2015; Wu et al., 2003), the expression pattern of MSX2 was unaltered in $Gli3^{\Delta 699/\Delta 699}$ and $Gli3^{XtJ/XtJ}$ eyes (Fig. 6B). Based on the fact that *Dkk1* is a target of β-CATENIN (Niida et al., 2004), it is possible that GLI3-R regulates the expression of *Dkk1* via a feedback loop that is triggered by the GLI3-R-mediated repression of *β-Catenin* expression (Ulloa et al., 2007) (Fig. 7).

Our study clearly demonstrates that GLI3-R but not GLI3-A is essential for vertebrate eye development and we hypothesise that GLI3-R ensures proper eye development by controlling WNT/β-CATENIN signalling. Since several other signalling pathways (like for example BMP, FGF and VEGF signalling) act downstream of HH signalling in eye development (Iwata and Hevner, 2009; Liu et al., 2018; Surace et al., 2006; Zhao et al., 2010), it is questionable whether the regulation of WNT/β-CATENIN signalling is the only mechanism which is governed by GLI3-R to assure proper eye development. In mice, a disturbed BMP signalling has been elucidated as a cause of a defective retinal development (Murali et al., 2005), microphthalmia (Liu et al., 2010; Okada et al., 2011) and anophthalmia (Dudley et al., 1995; Karsenty et al., 1996), an impaired FGF signalling has been shown to provoke the formation of coloboma (Atkinson-Leadbeater et al., 2014; Cai et al., 2013; Chen et al., 2013) and a perturbed VEGF signalling has been identified as a reason for the occurrence of microphthalmia (Rutland et al., 2007). Since these eye defects are also observed in $Gli3^{XtJ/XtJ}$ eyes, it is conceivable that GLI3-R controls eye development by regulating these signalling pathways in addition to the WNT/β-CATENIN pathway. Future studies in which β-CATENIN is knocked down in $Gli3^{XtJ/XtJ}$ eyes (e.g. by mating $Gli3^{XtJ/+}$ mice with inducible miRNA expressing knockdown mice) could provide valuable insights into this issue and hence make a substantial contribution to unravel the relationships between signalling cascades known to be essential for the development of the vertebrate eye.

4. Materials and methods

4.1. Ethics statement and animal husbandry

All mice (*Mus musculus*) used in this study were either on the B6C3F1 background ($Gli3^{XtJ}$) or on the C3H background ($Gli3^{\Delta 699}$) and kept under standard housing conditions with a 12/12 h dark-light cycle and food and

water *ad libitum*. All animal procedures were carried out in accordance with National Institutes of Health guidelines and with local and state regulations for research with animals.

4.2. Mouse strains

Gli3^{XtJ} mutant mice and *Gli3*$^{\Delta 699}$ mutant mice have been described previously (Böse et al., 2002; Franz and Besecke, 1991; Johnson, 1967). Genotypes were determined with PCR amplification of total genomic DNA, using 2 pairs of primers respectively.

For *Gli3*^{XtJ} following primers were used:

WT strand forward 5′-GGCCCAAACATCTACCAACACATAG-3′;
WT strand reverse 5′-GTTGGCTGCTGCATGAAGACTGAC-3′; deleted strand forward 5′-TACCCCAGCAGGAGACTCAGATTAG-3′;
deleted strand reverse 5′-AAACCCGTGGCTCAGGACAAG-3′.

For *Gli3*$^{\Delta 699}$ following primers were used:

WT strand forward 5′-GGCCCAAACATCTACCAACACATA-3′;
WT strand reverse 5′-CTGGCCACACTGAAAGGAAAAGAA-3′; deleted strand forward 5′-GATGCGGCGGTGGTAATGAC-3′;
deleted strand reverse 5′-TGTGTCTGTCCTCCGGAAGG-3′.

4.3. Antibodies

The following primary antibodies were used: anti-phospho Histone H3 (Ser10) (06-570; EMD Millipore), anti-OTX2 (AF1979; R&D Systems), anti-SOX1 (AF3369; R&D Systems), anti-SOX2 (AB5603; EMD Millipore), anti-PAX2 (901001; BioLegend), anti-β-CATENIN (PY489; Developmental Studies Hybridoma Bank), anti-MSX2 (sc-365232; Santa Cruz Biotechnology) and anti-DKK1 (kindly provided by Christof Niehrs, IMB Mainz).

4.4. Histology

Embryos at embryonic stages E14.5 and E18.5 or embryonic eyes were dissected and images were taken immediately. Afterwards the embryos were fixed in 4% paraformaldehyde (PFA) overnight at 4 °C. On the next day, they were gradually dehydrated using ethanol and embedded in paraffin. 12 µm sections were prepared. The sections were stained with haematoxylin and eosin (HE).

4.5. Image acquisition

Morphology and HE staining images were obtained using the Zeiss Axioskop 2 system, an AxioCam MRc (Carl Zeiss AG) and the AxioVision Rel. 4.7.1 software package (Carl Zeiss AG). Fluorescence image acquisition and data analysis were performed at room temperature using a Zeiss Imager.A2 microscope, 20x, NA 0.5 objective lens (Carl Zeiss AG), a monochrome charge-coupled device camera (AxioCam MRm; Carl Zeiss), and the AxioVision Rel. 4.8 software package (Carl Zeiss AG). Cy3 and Alexa488 were used as fluorochromes. Cell counting was performed by using Fiji (ImageJ; National Institutes of Health).

4.6. Immunofluorescence

Embryos at embryonic stage E12.5 were dissected, fixed in 4% PFA for 1.5 h and incubated in 30% sucrose (in PBS) overnight at 4 °C. The samples were embedded in Tissue-Tek O.C.T. compound (Sakura Finetechnical #4583) and freezed at −80 °C. Transverse cryostat sections (7 µm) were prepared and washed with PBS. A permeabilisation with PBS/0.5% Triton X-100 was performed. After three washing steps with PBS/0.1% Triton X-100 blocking was realised by incubation in 10% donkey serum in PBST. The sections then underwent an incubation in the primary antibodies diluted in PBS/0.1% Triton X-100 overnight at 4 °C. After overnight incubation the paraffin- and cryosections were washed three times, they were incubated with the secondary antibody (diluted in PBS/0.1% Triton X-100) for 2 h and were washed again. Finally, they were embedded in Mowiol optionally containing DAPI (Merck #1.24653).

4.7. In situ hybridisation

For immunofluorescence on paraffin-sections, embryos at embryonic stage E12.5 were dissected and fixed in 4% PFA overnight at 4 °C. On the next day, they were gradually dehydrated using ethanol and embedded in paraffin. 12 µm sections were prepared. *In situ* hybridisations were performed as previously described (Lieven and Rüther, 2011). The following probes were used: *Pax6*, *Pax2*, *Six3*, *Vax2* and *Wnt3a*.

4.8. Microarray

Transcriptome analyses were performed from samples of three mice strains. RNA was quantified by fluorometric Qubit assay (RNA HS; ThermoFisher scientific) measurement and quality measured by capillary electrophoresis Bioanalyzer assay (Eukaryote Total RNA Nano; Agilent). All samples in this study showed high quality RNA Integrity Numbers (RIN; median = 10) (Fig. S3). Synthesis of cDNA and subsequent biotin labeling of cRNA was performed according to the manufacturer's protocol (GeneChip® WT PLUS Reagent Kit 902462; ThermoFisher scientific). Briefly, 100 ng of total RNA were converted to cDNA, followed by in vitro transcription and biotin labeling of cDNA. After fragmentation labeled cDNA was hybridized to Affymetrix Mouse Gene 2.0 ST Gene Expression Microarrays for 16 h at 45 °C, stained by strepatavidin/phycoerythrin conjugate, and scanned as described in the manufacturer's protocol.

4.9. Statistical analysis

Data analyses on Affymetrix CEL files were conducted with GeneSpring GX software (Vers. 12.5; Agilent Technologies). Probes within each probe set were summarized by GeneSprings' ExonRMA16 algorithm after quantile normalization of probe-level signal intensities across all samples to reduce interarray variability (Bolstad et al., 2003). Input data preprocessing was concluded by baseline transformation to the median of all samples. After grouping of samples (three biological replicates each) according to their respective experimental condition, a given probe set had to be expressed above background (i.e., fluorescence signal of that probe set was detected within the 20th and 100th percentiles of the raw signal distribution of a given array) in all three replicates in at least one of three conditions to be further analysed in pairwise comparisons.

4.10. qRT-PCR

RNA was isolated from mouse embryonic eyes at E18.5 by using the RNeasy Kit (74104; Qiagen) and RNase-Free DNase Set (79254; Qiagen). Isolated RNA was converted into cDNA by QuantiTect Reverse Transcription Kit (205311; Qiagen). Quantitative real-time PCR was performed using a Step One Real-Time PCR System Thermal Cycling Block (4376357; Applied Biosystems) and a Maxima SYBR Green/ROX qPCR Master Mix 2x (K0222; Thermo Scientific). The following primer sets were used: *Dkk1* (forward 5′-ATATCACACCAAAGGACAAG-3′; reverse 5′-CCTTCTTTAAGGACAGGTTTAC-3′); *Foxe3* (forward 5′-ATCTACCGCTTCATCACC-3′; reverse 5′-ATCTACCGCTTCATCACC-3′); *Hes1* (forward 5′-AAGCCTATCATGGAGAAGAG-3′; reverse 5′-GGAGCTATCTTTCTTAAGTGC-3′); *Pax2* (forward 5′-ACAAGATTGCCGAATACAAG-3′; reverse 5′-GATGATCCTGTTGATGGATG-3′); *Six3* (forward 5′-CCACTGCTCCCTACTTCTGG-3′; reverse 5′-GCAACTGGAACATGGACAAC-3′); *Smoc1* (forward 5′-CCTTATGGATTAAGCACTTGG-3′; reverse 5′-TCACAGGAATGGACTTTCTC-3′) and *Tbx5* (forward 5′-CCAGAATCACAAGATCACAC-3′; reverse 5′-GGATACTCTTTACTTTGCATCC-3′). Real-time PCR was carried out with 50 ng of embryonic cDNA of each sample in triplicate reactions in a 25 µl volume containing 100 nM primers and 50 nM probe. Cycling conditions were 50 °C for 2 min and 95 °C for

10 min, followed by a 40-cycle amplification of 95 °C for 15 s, 60 °C for 30 s and 72 °C for 30s. The analysis of real-time data was performed by using included StepOne Software version 2.0.

4.11. Statistical data

Data are presented as mean ± standard error of mean (SEM). Analysis of variance (ANOVA) and Tukey honest significance difference (HSD) tests were performed for all data using GraphPad Prism (GraphPad Software). A P-value < 0.05 was regarded to be statistically significant (one asterisk), a P-value < 0.01 was accounted as statistically very significant (two asterisks), and a P-value < 0.001 was considered statistically high significant (three asterisks).

Competing interests

The authors declare no competing financial interests.

Funding

This work was supported by the Deutsche Forschungsgemeinschaft (Sonderforschungsbereiche 590 and 612) to U. R.

Acknowledgements

We thank Dr. Sylvie Schneider-Maunoury for critical reading of the manuscript and Dr. René Deenen for his assistance in the microarray analysis. Moreover, we are indebted to Dr. Karl W. Kafitz, Dr. Niklas J. Gerkau and Dr. Behrouz Moshrefi for their help regarding microscopy. Furthermore, we are grateful to Dr. Christof Niehrs for providing the anti-DKK1 antibody. The antibody against β-CATENIN developed by Dr. Janne Balsamo and Jack Lilien was obtained from the Developmental Studies Hybridoma Bank developed under the auspices of the NICHD and maintained by The University of Iowa, Department of Biological Sciences, Iowa City, IA 52242.

Appendix A. Supplementary data

Supplementary data to this article can be found online at https://doi.org/10.1016/j.ydbio.2019.02.018.

References

Aldahmesh, M., Mohammed, J., Al-Hazzaa, S., Alkuraya, F., 2012. Homozygous null mutation in ODZ3 causes microphthalmia in humans. Genet. Med. 14, 900–904.
Amato, M., Boy, S., Perron, M., 2004. Hedgehog signaling in vertebrate eye development: a growing puzzle. Cell. Mol. Life Sci. 61, 899–910.
Andley, U., Hamilton, P., Ravi, N., Weihl, C., 2011. A knock-in mouse model for the R120G mutation of αB-crystallin recapitulates human hereditary myopathy and cataracts. PLoS One 6, e17671.
Andreu-Cervera, A., Anselme, I., Karam, A., Laclef, C., Catala, M., Schneider-Maunoury, S., 2019. The ciliopathy gene ftm/rpgrip1l controls mouse forebrain patterning via region-specific modulation of hedgehog/gli signaling. J. Neurosci. pii: 2199-2118. [Epub ahead of print].
Aoto, K., Nishimura, T., Eto, K., Motoyama, J., 2002. Mouse GLI3 regulates Fgf8 expression and apoptosis in the developing neural tube, face, and limb bud. Dev. Biol. 251, 320–332.
Atkinson-Leadbeater, K., Hehr, C., Mcfarlane, S., 2014. Fgfr signaling is required as the early eye field forms to promote later patterning and morphogenesis of the eye. Dev. Dynam. 243, 663–675.
Bafico, A., Liu, G., Yaniv, A., Gazit, A., Aaronson, S., 2001. Novel mechanism of Wnt signalling inhibition mediated by Dickkopf-1 interaction with LRP6/Arrow. Nat. Cell Biol. 3, 683–686.
Bai, C., Stephen, D., Joyner, A., 2004. All mouse ventral spinal cord patterning by hedgehog is Gli dependent and involves an activator function of Gli3. Dev. Cell 6, 103–115.
Bakthavachalu, B., Kalanke, S., Galande, S., Ramanamurthy, B., Parab, P., Kohale, K., Seshadri, V., 2010. Dense cataract and microphthalmia (dcm) in BALB/c mice is caused by mutations in the GJA8 locus. J. Genet. 89, 147–154.
Bangs, F., Anderson, K., 2017. Primary cilia and mammalian hedgehog signaling. Cold Spring Harb. Perspect. Biol. 9, a028175.
Barbieri, A., Broccoli, V., Bovolenta, P., Alfano, G., Marchitiello, A., Mocchetti, C., Crippa, L., Bulfone, A., Marigo, V., Ballabio, A., Banfi, S., 2002. *Vax2* inactivation in mouse determines alteration of the eye dorsal-ventral axis, misrouting of the optic fibres and eye coloboma. Development 129, 805–813.
Barishak, Y., 1992. Embryology of the eye and its adnexae. Dev. Ophthalmol. 24, 1–142.
Bassett, E., Pontoriero, G., Feng, W., Marquardt, T., Fini, M., Williams, T., West-Mays, J., 2007. Conditional deletion of activating protein 2alpha (AP-2alpha) in the developing retina demonstrates non-cell-autonomous roles for AP-2alpha in optic cup development. Mol. Cell Biol. 27, 7497–7510.
Behesti, H., Holt, J., Sowden, J., 2006. The level of BMP4 signaling is critical for the regulation of distinct T-box gene expression domains and growth along the dorso-ventral axis of the optic cup. BMC Dev. Biol. 6, 62.
Behesti, H., Papaioannou, V., Sowden, J., 2009. Loss of Tbx2 delays optic vesicle invagination leading to small optic cups. Dev. Biol. 333, 360–372.
Ben-Zur, T., Feige, E., Motro, B., Wides, R., 2000. The mammalian Odz gene family: homologs of a Drosophila pair-rule gene with expression implying distinct yet overlapping developmental roles. Dev. Biol. 217, 107–120.
Berry, V., Francis, P., Reddy, M., Collyer, D., Vithana, E., MacKay, I., Dawson, G., Carey, A., Moore, A., Bhattacharya, S., Quinlan, R., 2001. Alpha-B crystallin gene (CRYAB) mutation causes dominant congenital posterior polar cataract in humans. Am. J. Hum. Genet. 69, 1141–1145.
Besse, L., Neti, M., Anselme, I., Gerhardt, C., Rüther, U., Laclef, C., Schneider-Maunoury, S., 2011. Primary cilia control telencephalic patterning and morphogenesis via Gli3 proteolytic processing. Development 138, 2079–2088.
Bhanot, P., Brink, M., Samos, C., Hsieh, J., Wang, Y., Macke, J., Andrew, D., Nathans, J., Nusse, R., 1996. A new member of the frizzled family from Drosophila functions as a Wingless receptor. Nature 382, 225–230.
Blixt, A., Mahlapuu, M., Aitola, M., Pelto-Huikko, M., Enerbäck, S., Carlsson, P., 2000. A forkhead gene, FoxE3, is essential for lens epithelial proliferation and closure of the lens vesicle. Genes Dev. 14, 245–254.
Bolstad, A., Eiken, H., Rosenlund, B., Alarcón-Riquelme, M., Jonsson, R., 2003. Increased salivary gland tissue expression of Fas, Fas ligand, cytotoxic T lymphocyte-associated antigen 4, and programmed cell death 1 in primary Sjögren's syndrome. Arthritis Rheum. 48, 174–185.
Böse, J., Grotewold, L., Rüther, U., 2002. Pallister-Hall syndrome phenotype in mice mutant for Gli3. Hum. Mol. Genet. 11, 1129–1135.
Bozanić, D., Saraga-Babić, M., 2004. Cell proliferation during the early stages of human eye development. Anat. Embryol. (Berl) 208, 381–388.
Brownell, I., Dirksen, M., Jamrich, M., 2000. Forkhead Foxe3 maps to the dysgenetic lens locus and is critical in lens development and differentiation. Genesis 27, 81–93.
Burnett, J., Lupu, F., Eggenschwiler, J., 2017. Proper ciliary assembly is critical for restricting Hedgehog signaling during early eye development in mice. Dev. Biol. 430, 32–40.
Cai, Z., Tao, C., Li, H., Ladher, R., Gotoh, N., Feng, G., Wang, F., Zhang, X., 2013. Deficient FGF signaling causes optic nerve dysgenesis and ocular coloboma. Development 140, 2711–2723.
Cao, T., Wang, C., Yang, M., Wu, C., Wang, B., 2013. Mouse limbs expressing only the Gli3 repressor resemble those of Sonic hedgehog mutants. Dev. Biol. 379, 221–228.
Ceroni, F., Aguilera-Garcia, D., Chassaing, N., Bax, D., Blanco-Kelly, F., Ramos, P., Tarilonte, M., Villaverde, C., da Silva, L., Ballesta-Martínez, M., Sanchez-Soler, M., Holt, R., Cooper-Charles, L., Bruty, J., Wallis, Y., McMullan, D., Hoffman, J., Bunyan, D., Stewart, A., Stewart, H., Lachlan, K., Study, D., Fryer, A., McKay, V., Roume, J., Dureau, P., Saggar, A., Griffiths, M., Calvas, P., Ayuso, C., Corton, M., Ragge, N., 2018. New GJA8 variants and phenotypes highlight its critical role in a broad spectrum of eye anomalies. Hum. Genet. https://doi.org/10.1007/s00439-018-1875-2.
Chapman, D., Garvey, N., Hancock, S., Alexiou, M., Agulnik, S., Gibson-Brown, J., Cebra-Thomas, J., Bollag, R., Silver, L., Papaioannou, V., 1996. Expression of the T-box family genes, Tbx1-Tbx5, during early mouse development. Dev. Dynam. 206, 379–390.
Chassaing, N., Ragge, N., Plaisancié, J., Patat, O., Geneviève, D., Rivier, F., Malrieu-Eliaou, C., Hamel, C., Kaplan, J., Calvas, P., 2016. Confirmation of TENM3 involvement in autosomal recessive colobomatous microphthalmia. Am. J. Med. Genet. A. 170, 1895–1898.
Chen, J., Laclef, C., Moncayo, A., Snedecor, E., Yang, N., Li, L., Takemaru, K., Paus, R., Schneider-Maunoury, S., Clark, R., 2015. The ciliopathy gene Rpgrip1l is essential for hair follicle development. J. Invest. Dermatol. 135, 701–709.
Chen, S., Li, H., Gaudenz, K., Paulson, A., Guo, F., Trimble, R., Peak, A., Seidel, C., Deng, C., Furuta, Y., Xie, T., 2013. Defective FGF signaling causes coloboma formation and disrupts retinal neurogenesis. Cell Res. 23, 254–273.
Chiang, C., Litingtung, Y., Lee, E., Young KE, C.J., Westphal, H., Beachy, P.A., 1996. Cyclopia and defective axial patterning in mice lacking Sonic hedgehog gene function. Nature 383, 407–413.
Choi, J., Ting, C., Trogrlic, L., Milevski, S., Familari, M., Martinez, G., de Iongh, R., 2014. A role for smoothened during murine lens and cornea development. PLoS One 9, e108037.
Cvekl, A., Zhang, X., 2017. Signaling and gene regulatory networks in mammalian lens development. Trends Genet. 33, 677–702.
Dakubo, G., Wang, Y., Mazerolle, C., Campsall, K., McMahon, A., Wallace, V., 2003. Retinal ganglion cell-derived sonic hedgehog signaling is required for optic disc and stalk neuroepithelial cell development. Development 130, 2967–2980.
de Verdier, K., Ulla, E., Löfgren, S., Fernell, E., 2017. Children with blindness - major causes, developmental outcomes and implications for habilitation and educational support: a two-decade, Swedish population-based study. Acta Ophthalmol. 96, 295–300.
Delous, M., Baala, L., Salomon, R., Laclef, C., Vierkotten, J., Tory, K., Golzio, C., Lacoste, T., Besse, L., Ozilou, C., Moutkine, I., Hellman, N., Anselme, I., Silbermann, F., Vesque, C., Gerhardt, C., Rattenberry, E., Wolf, M., Gubler, M.,

Martinovic, J., Encha-Razavi, F., Boddaert, N., Gonzales, M., Macher, M., Nivet, H., Champion, G., Berthélémé, J., Niaudet, P., McDonald, F., Hildebrandt, F., Johnson, C., Vekemans, M., Antignac, C., Rüther, U., Schneider-Maunoury, S., Attié-Bitach, T., Saunier, S., 2007. The ciliary gene RPGRIP1L is mutated in cerebello-oculo-renal syndrome (Joubert syndrome type B) and Meckel syndrome. Nat. Genet. 39, 875–881.
Dudley, A., Lyons, K., Robertson, E., 1995. A requirement for bone morphogenetic protein-7 during development of the mammalian kidney and eye. Genes Dev. 9, 2795–2807.
Dupé, V., Matt, N., Garnier, J., Chambon, P., Mark, M., Ghyselinck, N., 2003. A newborn lethal defect due to inactivation of retinaldehyde dehydrogenase type 3 is prevented by maternal retinoic acid treatment. Proc. Natl. Acad. Sci. U S A. 100, 14036–14041.
Fedi, P., Bafico, A., Nieto Soria, A., Burgess, W., Miki, T., Bottaro, D., Kraus, M., Aaronson, S., 1999. Isolation and biochemical characterization of the human Dkk-1 homologue, a novel inhibitor of mammalian Wnt signaling. J. Biol. Chem. 274, 19465–19472.
Franz, T., Besecke, A., 1991. The development of the eye in homozygotes of the mouse mutant Extra-toes. Anat. Embryol. (Berl.) 184, 355–361.
Fu, X., Sun, H., Klein, W., Mu, X., 2006. Beta-catenin is essential for lamination but not neurogenesis in mouse retinal development. Dev. Biol. 299, 424–437.
Fuhrmann, S., 2008. Wnt signaling in eye organogenesis. Organogenesis 4, 60–67.
Fuhrmann, S., 2010. Eye morphogenesis and patterning of the optic vesicle. Curr. Top. Dev. Biol. 93, 61–84.
Fujimura, N., 2016. WNT/β-Catenin signaling in vertebrate eye development. Front. Cell Dev. Biol. 4, 138.
Fujimura, N., Taketo, M., Mori, M., Korinek, V., Kozmik, Z., 2009. Spatial and temporal regulation of Wnt/beta-catenin signaling is essential for development of the retinal pigment epithelium. Dev. Biol. 334, 31–45.
Furimsky, M., Wallace, V., 2006. Complementary Gli activity mediates early patterning of the mouse visual system. Dev. Dynam. 235, 594–605.
Gerhardt, C., Leu, T., Lier, J., Rüther, U., 2016a. The cilia-regulated proteasome and its role in the development of ciliopathies and cancer. Cilia 5, 14.
Gerhardt, C., Lier, J., Burmühl, S., Struchtrup, A., Deutschmann, K., Vetter, M., Leu, T., Reeg, S., Grune, T., Rüther, U., 2015. The transition zone protein Rpgrip1l regulates proteasomal activity at the primary cilium. J. Cell Biol. 210, 115–133.
Gerhardt, C., Lier, J., Kuschel, S., Rüther, U., 2013. The ciliary protein Ftm is required for ventricular wall and septal development. PLoS One 8, e57545.
Gerhardt, C., Wiegering, A., Leu, T., Rüther, U., 2016b. Control of Hedgehog signalling by the cilia-regulated proteasome. J. Dev. Biol. 4, 27.
Glinka, A., Wu, W., Delius, H., Monaghan, A., Blumenstock, C., Niehrs, C., 1998. Dickkopf-1 is a member of a new family of secreted proteins and functions in head induction. Nature 391, 357–362.
Gogate, P., Gilbert, C., Zin, A., 2011. Severe visual impairment and blindness in infants: causes and opportunities for control. Middle East Afr. J. Ophthalmol. 18, 109–114.
Graw, J., 2003. The genetic and molecular basis of congenital eye defects. Nat. Rev. Genet. 4, 876–888.
Graw, J., 2009a. Genetics of crystallins: cataract and beyond. Exp. Eye Res. 88, 173–189.
Graw, J., 2009b. Mouse models of cataract. J. Genet. 88, 469–486.
Gregory-Evans, C., Wallace, V., Gregory-Evans, K., 2013. Gene networks: dissecting pathways in retinal development and disease. Prog. Retin. Eye Res. 33, 40–66.
Hägglund, A., Berghard, A., Carlsson, L., 2013. Canonical Wnt/β-catenin signalling is essential for optic cup formation. PLoS One 8, e81158.
He, F., Akbari, P., Mo, R., Zhang, J., Hui, C., Kim, P., Farhat, W., 2016. Adult Gli2+/-; Gli3Δ699/+ male and female mice display a spectrum of genital malformation. PLoS One 11, e0165958.
Hever, A., Williamson, K., van Heyningen, V., 2006. Developmental malformations of the eye: the role of PAX6, SOX2 and OTX2. Clin. Genet. 69, 459–470.
Hill, P., Götz, K., Rüther, U., 2009. A SHH-independent regulation of Gli3 is a significant determinant of anteroposterior patterning of the limb bud. Dev. Biol. 328, 506–516.
Ingham, P., McMahon, A., 2001. Hedgehog signaling in animal development: paradigms and principles. Genes Dev. 15, 3059–3087.
Iwata, T., Hevner, R., 2009. Fibroblast growth factor signaling in development of the cerebral cortex. Dev. Growth Differ. 51, 299–323.
Jacob, J., Briscoe, J., 2003. Gli proteins and the control of spinal-cord patterning. EMBO Rep. 4, 761–765.
Jiao, X., Khan, S., Irum, B., Khan, A., Wang, Q., Kabir, F., Khan, A., Husnain, T., Akram, J., Riazuddin, S., Hejtmancik, J., Riazuddin, S., 2015. Missense mutations in CRYAB are liable for recessive congenital cataracts. PLoS One 10, e0137973.
Johnson, D., 1967. Extra-toes: a new mutant gene causing multiple abnormalities in the mouse. J. Embryol. Exp. Morphol. 17, 543–581.
Kahn, B., Corman, T., Lovelace, K., Hong, M., Krauss, R., Epstein, D., 2017. Prenatal ethanol exposure in mice phenocopies Cdon mutation by impeding Shh function in the etiology of optic nerve hypoplasia. Dis. Model. Mech. 10, 29–37.
Kamachi, Y., Uchikawa, M., Collignon, J., Lovell-Badge, R., Kondoh, H., 1998. Involvement of Sox1, 2 and 3 in the early and subsequent molecular events of lens induction. Development 125, 2521–2532.
Karsenty, G., Luo, G., Hofmann, C., Bradley, A., 1996. BMP 7 is required for nephrogenesis, eye development, and skeletal patterning. Ann. N. Y. Acad. Sci. 785, 98–107.
Kerscher, S., Church, R., Boyd, Y., Lyon, M., 1995. Mapping of four mouse genes encoding eye lens-specific structural, gap junction, and integral membrane proteins: cryba1 (crystallin beta A3/A1), Crybb2 (crystallin beta B2), Gja8 (MP70), and Lim2 (MP19). Genomics 29, 445–450.
Khan, A., Abu Safieh, L., Alkuraya, F., 2010. Later retinal degeneration following childhood surgical aphakia in a family with recessive CRYAB mutation (p.R56W). Ophthalmic Genet. 31, 30–36.
Khan, A., Aldahmesh, M., Alkuraya, F., 2015. Phenotypes of recessive pediatric cataract in a cohort of children with identified homozygous gene mutations (an American ophthalmological society thesis). Trans. Am. Ophthalmol. Soc. 113, T7.
Kim, J., Lemke, G., 2006. Hedgehog-regulated localization of Vax2 controls eye development. Genes Dev. 20, 2833–2847.
Koshiba-Takeuchi, K., Takeuchi, J., Matsumoto, K., Momose, T., Uno, K., Hoepker, V., Ogura, K., Takahashi, N., Nakamura, H., Yasuda, K., Ogura, T., 2000. Tbx5 and the retinotectum projection. Science 287, 134–137.
Krämer, A., Green, J., Pollard, J.J., Tugendreich, S., 2014. Causal analysis approaches in ingenuity pathway analysis. Bioinformatics 30, 523–530.
Kreslova, J., Machon, O., Ruzickova, J., Lachova, J., Wawrousek, E., Kemler, R., Krauss, S., Piatigorsky, J., Kozmik, Z., 2007. Abnormal lens morphogenesis and ectopic lens formation in the absence of beta-catenin function. Genesis 45, 157–168.
Kumar, J., 2001. Signalling pathways in Drosophila and vertebrate retinal development. Nat. Rev. Genet. 2, 846–857.
Kumar, M., Agarwal, T., Khokhar, S., Kumar, M., Kaur, P., Roy, T., Dada, R., 2011. Mutation screening and genotype phenotype correlation of α-crystallin, γ-crystallin and GJA8 gene in congenital cataract. Mol. Vis. 17, 693–707.
Kurose, H., Bito, T., Adachi, T., Shimizu, M., Noji, S., Ohuchi, H., 2004. Expression of Fibroblast growth factor 19 (Fgf19) during chicken embryogenesis and eye development, compared with Fgf15 expression in the mouse. Gene Expr. Patterns 4, 687–693.
Lallemand, Y., Bensoussan, V., Cloment, C., Robert, B., 2009. Msx genes are important apoptosis effectors downstream of the Shh/Gli3 pathway in the limb. Dev. Biol. 331, 189–198.
Leamey, C., Merlin, S., Lattouf, P., Sawatari, A., Zhou, X., Demel, N., Glendining, K., Oohashi, T., Sur, M., Fässler, R., 2007. Ten_m3 regulates eye-specific patterning in the mammalian visual pathway and is required for binocular vision. PLoS Biol. 5, e241.
Lee, H., Wroblewski, E., Philips, G., Stair, C., Conley, K., Reedy, M., Mastick, G., Brown, N., 2005. Multiple requirements for Hes 1 during early eye formation. Dev. Biol. 284, 464–478.
Lee, M., Goraya, N., Kim, S., Cho, S., 2018. Hippo-yap signaling in ocular development and disease. Dev. Dynam. 247, 794–806.
Lei, Q., Zelman, A., Kuang, E., Li, S., Matise, M., 2004. Transduction of graded Hedgehog signaling by a combination of Gli2 and Gli3 activator functions in the developing spinal cord. Development 131, 3593–3604.
Li, J., Wang, C., Pan, Y., Bai, Z., Wang, B., 2011. Increased proteolytic processing of full-length Gli2 transcription factor reduces the hedgehog pathway activity in vivo. Dev. Dynam. 240, 766–774.
Li, Y., Lin, H., 2013. Progress in screening and treatment of common congenital eye diseases. Eye Sci. 28, 157–162.
Lieven, O., Dronka, J., Burmühl, S., Rüther, U., 2014. Differential binding of Lef1 and Msx1/2 transcription factors to Dkk1 CNEs correlates with reporter gene expression in vivo. PLoS One 9, e115442.
Lieven, O., Rüther, U., 2011. The Dkk1 dose is critical for eye development. Dev. Biol. 355, 124–137.
Liu, M., Chen, X., Liu, H., Di, Y., 2018. Expression and significance of the Hedgehog signal transduction pathway in oxygen-induced retinal neovascularization in mice. Drug Des. Dev. Ther. 12, 1337–1346.
Liu, W., Lagutin, O., Mende, M., Streit, A., Oliver, G., 2006. Six3 activation of Pax6 expression is essential for mammalian lens induction and specification. EMBO J. 25, 5383–5395.
Liu, Y., Kawai, K., Khashabi, S., Deng, C., Liu, Y., Yiu, S., 2010. Inactivation of Smad4 leads to impaired ocular development and cataract formation. Biochem. Biophys. Res. Commun. 400, 476–482.
Ludwig, P., Czyz, C., 2017. Embryology, Eye, Malformations [Internet]. StatPearls, Treasure Island (FL).
Lupu, F., Burnett, J., Eggenschwiler, J., 2018. Cell cycle-related kinase regulates mammalian eye development through positive and negative regulation of the Hedgehog pathway. Dev. Biol. 434, 24–35.
Mahuzier, A., Gaudé, H., Grampa, V., Anselme, I., Silbermann, F., Leroux-Berger, M., Delacour, D., Ezan, J., Montcouquiol, M., Saunier, S., Schneider-Maunoury, S., Vesque, C., 2012. Dishevelled stabilization by the ciliopathy protein Rpgrip1l is essential for planar cell polarity. J. Cell Biol. 198, 927–940.
Mao, B., Wu, W., Li, Y., Hoppe, D., Stannek, P., Glinka, A., Niehrs, C., 2001. LDL-receptor-related protein 6 is a receptor for Dickkopf proteins. Nature 411, 321–325.
Matt, N., Dupé, V., Garnier, J., Dennefeld, C., Chambon, P., Mark, M., Ghyselinck, N., 2005. Retinoic acid-dependent eye morphogenesis is orchestrated by neural crest cells. Development 132, 4789–4800.
McNeill, B., Perez-Iratxeta, C., Mazerolle, C., Furimsky, M., Mishina, Y., Andrade-Navarro, M., Wallace, V., 2012. Comparative genomics identification of a novel set of temporally regulated hedgehog target genes in the retina. Mol. Cell. Neurosci. 49, 333–340.
Medina-Martinez, O., Brownell, I., Amaya-Manzanares, F., Hu, Q., Behringer, R., Jamrich, M., 2005. Severe defects in proliferation and differentiation of lens cells in Foxe3 null mice. Mol. Cell Biol. 25, 8854–8863.
Medina-Martinez, O., Jamrich, M., 2007. Foxe view of lens development and disease. Development 134, 1455–1463.
Merlin, S., Horng, S., Marotte, L., Sur, M., Sawatari, A., Leamey, C., 2013. Deletion of Ten-m3 induces the formation of eye dominance domains in mouse visual cortex. Cerebr. Cortex 23, 763–774.
Mic, F., Molotkov, A., Fan, X., Cuenca, A., Duester, G., 2000. RALDH3, a retinaldehyde dehydrogenase that generates retinoic acid, is expressed in the ventral retina, otic vesicle and olfactory pit during mouse development. Mech. Dev. 97, 227–230.

Miller, L., Smith, A., Taketo, M., Lang, R., 2006. Optic cup and facial patterning defects in ocular ectoderm beta-catenin gain-of-function mice. BMC Dev. Biol. 6, 14.
Murali, D., Yoshikawa, S., Corrigan, R., Plas, D., Crair, M., Oliver, G., Lyons, K., Mishina, Y., Furuta, Y., 2005. Distinct developmental programs require different levels of Bmp signaling during mouse retinal development. Development 132, 913–923.
Niida, A., Hiroko, T., Kasai, M., Furukawa, Y., Nakamura, Y., Suzuki, Y., Sugano, S., Akiyama, T., 2004. DKK1, a negative regulator of Wnt signaling, is a target of the beta-catenin/TCF pathway. Oncogene 23, 8520–8526.
Nishiguchi, S., Wood, H., Kondoh, H., Lovell-Badge, R., Episkopou, V., 1998. Sox1 directly regulates gamma-crystallin genes and is essential for lens development in mice. Genes Dev. 12, 776–781.
Nishihara, D., Yajima, I., Tabata, H., Nakai, M., Tsukiji, N., Katahira, T., Takeda, K., Shibahara, S., Nakamura, H., Yamamoto, H., 2012. Otx2 is involved in the regional specification of the developing retinal pigment epithelium by preventing the expression of sox2 and fgf8, factors that induce neural retina differentiation. PLoS One 7, e48879.
Okada, I., Hamanoue, H., Terada, K., Tohma, T., Megarbane, A., Chouery, E., Abou-Ghoch, J., Jalkh, N., Cogulu, O., Ozkinay, F., Horie, K., Takeda, J., Furuichi, T., Ikegawa, S., Nishiyama, K., Miyatake, S., Nishimura, A., Mizuguchi, T., Niikawa, N., Hirahara, F., Kaname, T., Yoshiura, K., Tsurusaki, Y., Doi, H., Miyake, N., Furukawa, T., Matsumoto, N., Saitsu, H., 2011. SMOC1 is essential for ocular and limb development in humans and mice. Am. J. Hum. Genet. 88, 30–41.
Pan, Y., Bai, C., Joyner, A., Wang, B., 2006. Sonic hedgehog signaling regulates Gli2 transcriptional activity by suppressing its processing and degradation. Mol. Cell Biol. 26, 3365–3377.
Pineda-Alvarez, D., Solomon, B., Roessler, E., Balog, J., Hadley, D., Zein, W., Hadsall, C., Brooks, B., Muenke, M., 2011. A broad range of ophthalmologic anomalies is part of the holoprosencephaly spectrum. Am. J. Med. Genet. A. 155A, 2713–2720.
Pinson, K., Brennan, J., Monkley, S., Avery, B., Skarnes, W., 2000. An LDL-receptor-related protein mediates Wnt signalling in mice. Nature 407, 535–538.
Plaisancié, J., Collet, C., Pelletier, V., Perdomo, Y., Studer, F., Fradin, M., Schaefer, E., Speeg-Schatz, C., Bloch-Zupan, A., Flori, E., Dollfus, H., 2015. MSX2 gene duplication in a patient with eye development defects. Ophthalmic Genet. 36, 353–358.
Rainger, J., van Beusekom, E., Ramsay, J., McKie, L., Al-Gazali, L., Pallotta, R., Saponari, A., Branney, P., Fisher, M., Morrison, H., Bicknell, L., Gautier, P., Perry, P., Sokhi, K., Sexton, D., Bardakjian, T., Schneider, A., Elcioglu, N., Ozkinay, F., Koenig, R., Mégarbané, A., Semerci, C., Khan, A., Zafar, S., Hennekam, R., Sousa, S., Ramos, L., Garavelli, L., Furga, A., Wischmeijer, A., Jackson, I., Gillessen-Kaesbach, G., Brunner, H., Wieczorek, D., van Bokhoven, H., Fitzpatrick, D., 2011. Loss of the BMP antagonist, SMOC-1, causes Ophthalmo-acromelic (Waardenburg Anophthalmia) syndrome in humans and mice. PLoS Genet. 7, e1002114.
Rallu, M., Machold, R., Gaiano, N., Corbin, J., McMahon, A., Fishell, G., 2002. Dorsoventral patterning is established in the telencephalon of mutants lacking both Gli3 and Hedgehog signaling. Development 129, 4963–4974.
Reis, L., Semina, E., 2015. Conserved genetic pathways associated with microphthalmia, anophthalmia, and coloboma. Birth Defects Res. C. Embryo Today 105, 96–113.
Ruiz i Altaba, A., 1999a. Gli proteins and Hedgehog signaling: development and cancer. Trends Genet. 15, 418–425.
Ruiz i Altaba, A., 1999b. The works of GLI and the power of hedgehog. Nat. Cell Biol. 1, E147–E148.
Ruiz i Altaba, A., Nguyên, V., Palma, V., 2003. The emergent design of the neural tube: prepattern, SHH morphogen and GLI code. Curr. Opin. Genet. Dev. 13, 513–521.
Ruiz i Altaba, A., Palma, V., Dahmane, N., 2002. Hedgehog-Gli signalling and the growth of the brain. Nat. Rev. Neurosci. 3, 24–33.
Russell, C., 2003. The roles of Hedgehogs and Fibroblast Growth Factors in eye development and retinal cell rescue. Vision Res. 43, 899–912.
Rutland, C., Mitchell, C., Nasir, M., Konerding, M., Drexler, H., 2007. Microphthalmia, persistent hyperplastic hyaloid vasculature and lens anomalies following overexpression of VEGF-A188 from the alphaA-crystallin promoter. Mol. Vis. 13, 47–56.
Sano, Y., Matsukane, Y., Watanabe, A., Sonoda, K., Kondo, H., 2018. Lack of FOXE3 coding mutation in a case of congenital aphakia. Ophthalmic Genet. 39, 95–98.
Sasaki, H., Nishizaki, Y., Hui, C., Nakafuku, M., Kondoh, H., 1999. Regulation of Gli2 and Gli3 activities by an amino-terminal repression domain: implication of Gli2 and Gli3 as primary mediators of Shh signaling. Development 126, 3915–3924.
Schimmang, T., Lemaistre, M., Vortkamp, A., Rüther, U., 1992. Expression of the zinc finger gene Gli3 is affected in the morphogenetic mouse mutant extra-toes (Xt). Development 116, 799–804.
Schwarz, M., Cecconi, F., Bernier, G., Andrejewski, N., Kammandel, B., Wagner, M., Gruss, P., 2000. Spatial specification of mammalian eye territories by reciprocal transcriptional repression of Pax2 and Pax6. Development 127, 4325–4334.
Semënov, M., Tamai, K., Brott, B., Kühl, M., Sokol, S., He, X., 2001. Head inducer Dickkopf-1 is a ligand for Wnt coreceptor LRP6. Curr. Biol. 11, 951–961.
Semenza, G., Wang, G., Kundu, R., 1995. DNA binding and transcriptional properties of wild-type and mutant forms of the homeodomain protein Msx2. Biochem. Biophys. Res. Commun. 209, 257–262.
Smith, A., Miller, L., Song, N., Taketo, M., Lang, R., 2005. The duality of beta-catenin function: a requirement in lens morphogenesis and signaling suppression of lens fate in periocular ectoderm. Dev. Biol. 285, 477–489.
Solebo, A., Teoh, L., Rahi, J., 2017. Epidemiology of blindness in children. Arch. Dis. Child. 102, 853–857.
Steele, E.J., Lyon, M., Favor, J., Guillot, P., Boyd, Y., Church, R., 1998. A mutation in the connexin 50 (Cx50) gene is a candidate for the No2 mouse cataract. Curr. Eye Res. 17, 883–889.
Struchtrup, A., Wiegering, A., Stork, B., Rüther, U., Gerhardt, C., 2018. The ciliary protein RPGRIP1L governs autophagy independently of its proteasome-regulating function at the ciliary base in mouse embryonic fibroblasts. Autophagy 14, 567–583.
Surace, E., Balaggan, K., Tessitore, A., Mussolino, C., Cotugno, G., Bonetti, C., Vitale, A., Ali, R., Auricchio, A., 2006. Inhibition of ocular neovascularization by hedgehog blockade. Mol. Ther. 13, 573–579.
Suzuki, R., Shintani, T., Sakuta, H., Kato, A., Ohkawara, T., Osumi, N., Noda, M., 2000. Identification of RALDH-3, a novel retinaldehyde dehydrogenase, expressed in the ventral region of the retina. Mech. Dev. 98, 37–50.
Takatsuka, K., Hatakeyama, J., Bessho, Y., Kageyama, R., 2004. Roles of the bHLH gene Hes1 in retinal morphogenesis. Brain Res. 1004, 148–155.
Take-uchi, M., Clarke, J., Wilson, S., 2003. Hedgehog signalling maintains the optic stalk-retinal interface through the regulation of Vax gene activity. Development 130, 955–968.
Tamai, K., Semenov, M., Kato, Y., Spokony, R., Liu, C., Katsuyama, Y., Hess, F., Saint-Jeannet, J., He, X., 2000. LDL-receptor-related proteins in Wnt signal transduction. Nature 407, 530–535.
Templeton, J., Wang, X., Freeman, N., Ma, Z., Lu, A., Hejtmancik, F., Geisert, E., 2013. A crystallin gene network in the mouse retina. Exp. Eye Res. 116, 129–140.
Tomita, K., Ishibashi, M., Nakahara, K., Ang, S., Nakanishi, S., Guillemot, F., Kageyama, R., 1996. Mammalian hairy and Enhancer of split homolog 1 regulates differentiation of retinal neurons and is essential for eye morphogenesis. Neuron 16, 723–734.
Traboulsi, E., 1998. Ocular malformations and developmental genes. J. AAPOS 2, 317–323.
Ulloa, F., Itasaki, N., Briscoe, J., 2007. Inhibitory Gli3 activity negatively regulates Wnt/beta-catenin signaling. Curr. Biol. 17, 545–550.
Verma, A., Fitzpatrick, D., 2007. Anophthalmia and microphthalmia. Orphanet J. Rare Dis. 2, 47.
Vierkotten, J., Dildrop, R., Peters, T., Wang, B., Rüther, U., 2007. Ftm is a novel basal body protein of cilia involved in Shh signalling. Development 134, 2569–2577.
Wall, D., Mears, A., McNeill, B., Mazerolle, C., Thurig, S., Wang, Y., Kageyama, R., Wallace, V., 2009. Progenitor cell proliferation in the retina is dependent on Notch-independent Sonic hedgehog/Hes1 activity. J. Cell Biol. 184, 101–112.
Wang, B., Fallon, J., Beachy, P., 2000. Hedgehog-regulated processing of Gli3 produces an anterior/posterior repressor gradient in the developing vertebrate limb. Cell 100, 423–434.
Wang, C., Rüther, U., Wang, B., 2007. The Shh-independent activator function of the full-length Gli3 protein and its role in vertebrate limb digit patterning. Dev. Biol. 305, 460–469.
Wang, E., Geng, A., Maniar, A., Mui, B., Gong, X., 2016. Connexin 50 regulates surface ball-and-socket structures and fiber cell organization. Invest. Ophthalmol. Vis. Sci. 57, 3039–3046.
Wang, J., Liu, Y., Su, Z., Pan, L., Lu, F., Qu, J., Hou, L., 2017. The T-box transcription factor TBX2 regulates cell proliferation in the retinal pigment epithelium. Curr. Eye Res. 42, 1537–1544.
Wehrli, M., Dougan, S., Caldwell, K., O'Keefe, L., Schwartz, S., Vaizel-Ohayon, D., Schejter, E., Tomlinson, A., DiNardo, S., 2000. Arrow encodes an LDL-receptor-related protein essential for Wingless signalling. Nature 407, 527–530.
Wiegering, A., Dildrop, R., Kalfhues, L., Spychala, A., Kuschel, S., Lier, J., Zobel, T., Dahmen, S., Leu, T., Struchtrup, A., Legendre, F., Vesque, C., Schneider-Maunoury, S., Saunier, S., Rüther, U., Gerhardt, C., 2018a. Cell type-specific regulation of ciliary transition zone assembly in vertebrates. EMBO J. 37, e97791.
Wiegering, A., Rüther, U., Gerhardt, C., 2017. The role of Hedgehog signalling in the formation of the ventricular septum. J. Dev. Biol. 5, 17.
Wiegering, A., Rüther, U., Gerhardt, C., 2018b. The ciliary protein Rpgrip1l in development and disease. Dev. Biol. 442, 60–68.
Willert, K., Nusse, R., 1998. Beta-catenin: a key mediator of Wnt signaling. Curr. Opin. Genet. Dev. 8, 95–102.
Williamson, K., FitzPatrick, D., 2014. The genetic architecture of microphthalmia, anophthalmia and coloboma. Eur. J. Med. Genet. 57, 369–380.
Wu, L., Li, M., Hinton, D., Guo, L., Jiang, S., Wang, J., Zeng, A., Xie, J., Snead, M., Shuler, C., Maxson, R.J., Liu, Y., 2003. Microphthalmia resulting from MSX2-induced apoptosis in the optic vesicle. Invest. Ophthalmol. Vis. Sci. 44, 2404–2412.
Zaki, P., Collinson, J., Toraiwa, J., Simpson, T., Price, D., Quinn, J., 2006. Penetrance of eye defects in mice heterozygous for mutation of Gli3 is enhanced by heterozygous mutation of Pax6. BMC Dev. Biol. 6, 46.
Zhao, L., Saitsu, H., Sun, X., Shiota, K., Ishibashi, M., 2010. Sonic hedgehog is involved in formation of the ventral optic cup by limiting Bmp4 expression to the dorsal domain. Mech. Dev. 127, 62–72.